Environmental Earth Sciences (2023) 82:345
https://doi.org/10.1007/s12665-023-11026-7

ORIGINAL ARTICLE

A new quantitative welding degree classification for ignimbrites

Mutluhan Akin[1] · Tamer Topal[2] · İsmail Dinçer[1] · Muge K. Akin[3] · Ali Özvan[4] · Ahmet Orhan[1] · Ayşe Orhan[1]

Received: 23 January 2023 / Accepted: 10 June 2023 / Published online: 28 June 2023

Abstract

As a pyroclastic rock type, ignimbrites may reveal varying degrees of welding depending on the temperature (> 535 ℃) and overburden pressure conditions during its formation. The welding degree of ignimbrites increases as the formation temperature and the thickness of the overburden deposit in the depositional environment escalate, which are the most crucial factors controlling the rate of welding in ignimbrites. With the increasing temperature, plastic deformation is observed in ignimbrites and the glassy minerals are being welded. Furthermore, the thickness of the overburden causes the deformation of the ash matrix in ignimbrites at the lower sections and the pumice grains are flattened at different rates. An increase in the degree of welding of ignimbrites causes an improvement in the physical and mechanical properties of the rock material as well. Within the scope of this research, petrographical, mineralogical, and geochemical studies were carried out on a total of 16 different ignimbrite types, which have different color and texture properties, obtained from three different regions of Turkey (Kayseri, Nevşehir, Ahlat) where ignimbrites extensively crop out, and the physical and mechanical properties of these samples were revealed. Consequently, a new welding classification was developed for ignimbrites considering the uniaxial compressive strength and dry unit weight. The proposed welding classification consists of six classes ranging from non-welded to highly welded. When the welding degrees of the selected ignimbrites are evaluated, Kayseri ignimbrites mostly exhibit moderate welding characteristics. Nevşehir ignimbrites, on the other hand, have a low welding degree whereas the degree of welding in Ahlat ignimbrites may vary from low to high. Additionally, long and short axis lengths of pumice grains in the ignimbrite specimens were determined by measuring under the microscope, and shape ratios were determined by different shape parameter evaluation methods. As a result, it has been concluded that the pumice grains in Kayseri and Ahlat ignimbrites have a more lenticular structure than the pumice grains in Nevşehir ignimbrites. Eventually, the welding degree classes of ignimbrites and the classification developed by using threshold values of the oblateness ratio (OR) values of pumice grains at different welding degrees are quite compatible. The proposed welding degree classification is of great importance in the selection of ignimbrites widely used as dimension stone and in terms of engineering classification of this rock type as well as it will guide to the scientific studies to be performed on ignimbrites with varying physical and mechanical properties.

Keywords Welding · Ignimbrite · Pumice · Welding degree classification · Oblateness ratio · Strength

Introduction

Ignimbrite is generally defined as a pyroclastic rock formed as a result of the deposition as well as cooling of hot (500–700 ℃) and intense pyroclastic flows, mostly composed of pumice and volcanic rock fragments (Walker 1983; Moon 1993). The temperature conditions during their accumulation and the overburden load in the depositional environment play major roles on the welding degree of ignimbrites. Ignimbrites formed under high temperature (> 550–600 ℃) and thick overburden layers exhibit relatively better physical and mechanical properties. Welding is associated with considerable changes in the texture, structure, and

✉ Mutluhan Akin
mutluhanakin@nevsehir.edu.tr

[1] Cappadocia Geological Heritage and Rock-Hewn Structures Application and Research Center, Department of Geological Engineering, Nevşehir Hacı Bektaş Veli University, Nevşehir, Turkey

[2] Department of Geological Engineering, Middle East Technical University, Ankara, Turkey

[3] Department of Civil Engineering, Abdullah Gul University, Kayseri, Turkey

[4] Department of Geological Engineering, Van Yüzüncü Yıl University, Van, Turkey

physical properties of pyroclastic deposits (Koralay et al. 2011). Therefore, the physical and mechanical properties of ignimbrites may vary in a wide range. In many scientific studies, it has been emphasized that there is certain relationship between the physical properties of ignimbrites and the degree of welding (Streck and Grunder 1995; Branney and Kokelaar, 2002; Quane and Russell 2005a, 2005b; Mundula et al. 2009; Koralay et al. 2011; Bozdağ et al. 2016; Korkanç and Solak 2016; Pola et al. 2016; Selçuk and Beyaz 2021). During the formation of ignimbrites, the pyroclastic material that erupts from the volcanic vents and flows along the slope includes rock fragments (lithic material) as well as pumice grains with very high porosity. Although the shape of the lithic material is not substantially affected by the formation temperatures of ignimbrite, in areas with high pyroclastic flow temperatures (> 600 ℃) and thick ignimbrite deposits, the pumice grains are flattened with the effect of high temperature forming lens-shaped fiamme structures and the rock texture is defined as eutaxitic (Fig. 1). For ignimbrites formed in such an environment, the strength of the rock material increases relatively, the porosity decreases, and as a result, the welding degree of the ignimbrites increases (Fig. 2) (Smith 1960; Moon 1993; Quane and Russell 2005b).

In scientific literature, although it is emphasized that the flattening of pumice grains increases with the increasing degree of welding, the relationship of oblateness with the physical and mechanical properties of the rock is not examined in detail. Furthermore, quantitative classifications that can be used to reveal the degree of welding of ignimbrites are very limited.

Braney and Kokelaar (1992) stated that ignimbrites can exhibit highly variable textural features in vertical and horizontal directions depending on their deposition characteristics, and the texture can be non-welded, eutaxitic, rheomorphic (lineated) and lava-type. The authors emphasized that the aspect ratio of fiamme structure is also related to the deposition, especially in highly welded ignimbrites, and

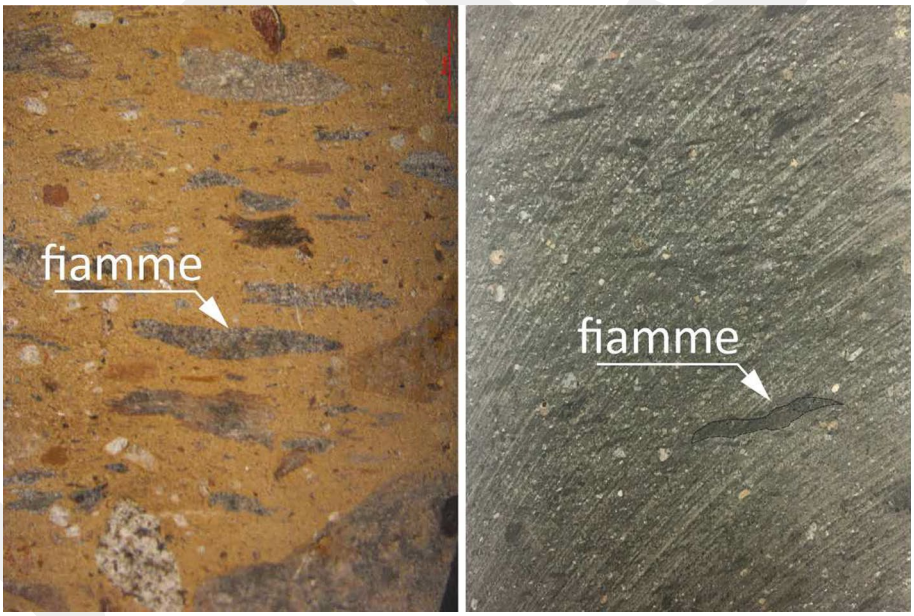

Fig. 1 Close-up views of lens-shaped fiamme structures in ignimbrites

Fig. 2 Schematic representation of the vertical and lateral distribution of welding zones in depositional environment of ignimbrites (modified after Smith 1960)

may not always indicate compaction. In addition, the textural features of ignimbrites reflect the deposition regime rather than the transport regime, and the granular and non-granular lineation indicates the deposition limits. The compressive strength and slake durability in ignimbrites substantially depend on the dispersion density of the glassy material in the matrix and the degree of welding at the contact points of the glassy materials. Conversely, crystal and grain size exert a secondary effect on the compressive strength, while tensile strength is related to the orientation of glass shards which are vitric fragments derived from the pulverization of pumice during eruption in ignimbrites (Moon 1993).

Streck and Grunder (1995) distinguished four facies of welding in Rattlesnake tuffs of Oregon namely non-welded, incipiently welded, partially welded and densely welded zones; as well as four post-emplacement crystallization phases such as vapor, pervasively devitrified, spherulite and lithophysae. No visible deformation is declared in the pumice grains and volcanic glass shards in the non-welded tuffs. Although there is no lineation or deformation in the lithic materials of the incipiently welded tuffs, the glass shards are partly bonded as a result of adhesion. The partially welded layers of tuffs are divided into a couple of zones with pumice and fiamme. The pumice grains are slightly deformed in the pumice-rich zones with very little coalescence of glass shards. Besides, the pumice grains transform into glassy fiamme in the partially welded zones with fiamme structures, but the matrix is still porous with an eutaxitic texture. Conversely, densely welded tuffs display a dark vitrophyric texture, obsidian-like and non-porous appearance. The eutaxitic texture disappeared with intense welding. Moreover, Streck and Grunder (1995) reported that the unit weight is less than 1.5 g/cm^3 in non-welded tuffs, whereas it is around 2.3 g/cm^3 in densely welded specimens. Welding degree of basaltic ignimbrites are classified as unwelded, poorly welded, moderately welded, strongly welded and densely welded by Freundt and Schmincke (1995) and it is stated that the particle shape changes from sub-spherical-oval to increasingly flattened with the escalated welding degree. Additionally, the bulk density of ignimbrites is much more affected by the degree of welding rather than the amount of crystals and lithic fragments (Mues-Schumacher et al. 2004). Welding degree of ignimbrites is also controlled by compaction welding after the pyroclastic flows and increases with the increasing overburden thickness, especially in the flows accumulating behind topographic elevations. Gifkins et al. (2005) studied fiamme structures in ignimbrites and emphasized that fiammes are deformation structures reflecting the eutaxitic texture in welded ignimbrites. The fiamme structure and eutaxitic texture are not only observed in welded ignimbrites, but can also be found in non-welded, pumice-rich pyroclastics. Nevertheless, the pumice grains are randomly oriented and the oblateness rate is very low in this type of pyroclastic deposits. The fiamme may reveal varying shapes such as flame-like, bow tie, irregular branching, wedge and blocky which have feathery or brush-like terminations and the length of fiamme can vary between 0.5 mm and 1 m with a length-to-height ratio range of 3:1 to 40:1 (Fig. 3). The oblateness ratio of fiamme revealing brush-like terminations is lower than the fiammes ending with long and thin stylolite (Gifkins et al. 2005).

During the welding of pyroclastic units, the glassy fragments are flattened as a result of the overburden load that exerts a compression effect and the temperatures above the glass transition temperature. Moreover, the petrographic and physical properties of the rock improve with progressive coalescence. Quane and Russell (2005a) classified the welding of pyroclastic rocks into 6 subclasses ranging from I to VI. While the rocks in Rank-I do not reveal any sign of welding, a vitrophyric texture similar to obsidian is dominant in welding Rank-VI. In the study carried out by Quane and Russell (2005a), the distribution of physical and mechanical properties of the rock at different degrees of welding is depicted in Table 1.

Rank-I in the classification scheme of Quane and Russell (2005a) corresponds to non-welded rocks with undeformed pumice fragments in a loosely-packed, unconsolidated matrix. The pyroclastic rock is still undeformed and some adhesion exists between the clasts in Rank-II indicating an incipiently welded pyroclastic rock. Slight deformation in the ash matrix and pumice fragments is noticeable in the rocks of Rank-III which can be assigned as partially or poorly welded. Rank-IV is characterized by moderately welded pyroclastic rocks with some fiamme structures. In contrast, in Rank-V, the oblateness ratio fiammes is very high and scatters in a strongly foliated ash matrix. Rank-VI type pyroclastic rocks reveal an obsidian-like vitrophyre texture as well as glass shards are completely distorted and adhered to one another (Quane and Russell 2005a). Finally, it is stated in the same study that the oblateness ratio of ignimbrites in low welding rank is commonly lower than 0.6 and it can be as high as 0.82 as a result of increasing welding. The determination coefficient between unit weight and oblateness ratio is reported to be 0.90 as well.

Mundula et al. (2009), in their study on different textures observed in ignimbrites, state that the welding degree of ignimbrites varies in a wide range and draw attention to the post-deposition crystallization in ignimbrites. A classification was developed by the researchers based on the aspect ratio (AR = a/c) (Sheridan and Ragan 1976), the orientation of the volcanic glass shards which is expressed by circular variance (Vc = 1 – (Rc/N)) (Tran 2007) and the style of crystallization of the matrix (Fig. 4). As the AR approaches 1, the shape of pumice grains is almost circular and with the escalation of AR ratio, they acquire an elliptical form. Furthermore, Vc is negatively associated with the orientation

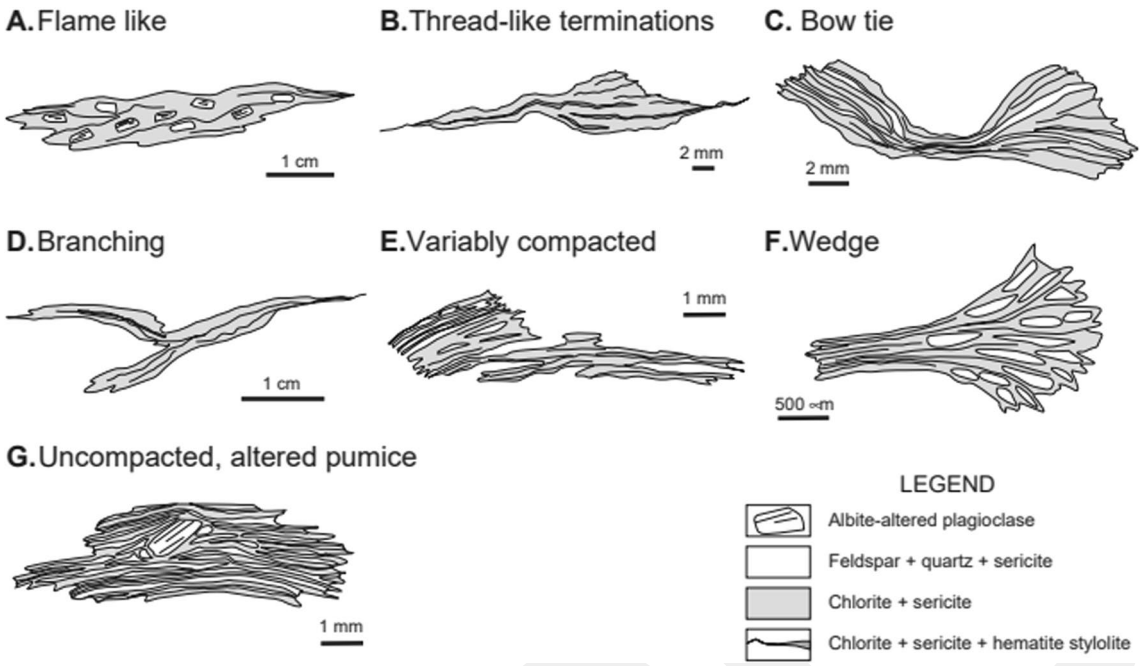

Fig. 3 Different fiamme shapes and textures of pumice fragments (after Gifkins et al. 2005)

Table 1 Variations in the physical and mechanical properties and oblateness ratios of different welding degrees in ignimbrites (Quane and Russell 2005a)

Rank	ε	ρ	ρ_n	f	PLST	UCS	OB	FA
I	< 0.31	< 1.45	< 0.60	> 0.42	< 0.59	< 4.4	< 0.50	> 33.2
II	0.2–0.39	1.25–1.65	0.49–0.67	0.50–0.34	0.28–1.13	1.8–9.8	0.46–0.67	40.4–28.0
III	0.39–0.47	1.65–1.85	0.67–0.76	0.34–0.25	1.13–2.15	9.8–21.4	0.67–0.74	28.0–23.7
IV	0.47–0.52	1.85–2.15	0.76–0.88	0.25–0.13	2.15–4.6	21.4–53.2	0.74–0.8	23.7–19.5
V	0.52–0.57	2.15–2.3	0.88–0.94	0.13–0.07	4.6–6.4	53.2–80.2	0.8–0.82	19.5–17.8
VI	> 0.57	> 2.3	> 0.94	< 0.07	> 6.4	> 80.2	> 0.82	< 17.8

ε Strain, *ρ* Density (g/cm^3), ρ_n Normalized density, *f* Porosity, *PLST* Point load strength (MPa), *UCS* Uniaxial compressive strength (MPa),*OB* Oblateness, *FA* Fabric angle

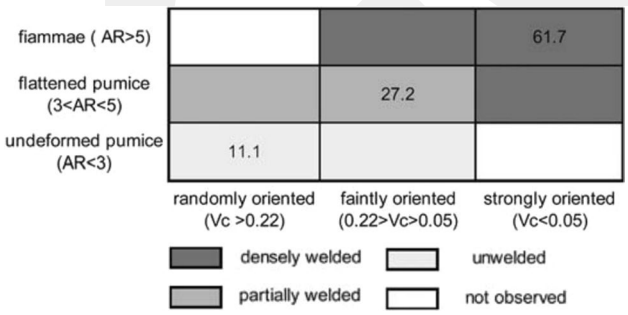

Fig. 4 Welding classification based on pumice shape and orientation of glass shards in ignimbrites (Mundula et al. 2009)

of glass shards and randomly orientation is expressed by a Vc value of higher than 0.22 whereas Vc lower than 0.05 defines strong glass shard orientation (Mundula et al. 2009).

The physical and mechanical properties of pyroclastic rocks are highly reliant on the welding degree (Korkanç and Solak 2016). Welding of pyroclastic rocks causes an increment in unit weight and strength, and a decrement in porosity (Koralay et al. 2011). On the other hand, ignimbrites with a high degree of welding resist freeze–thaw cycles better than partially welded specimens. Koralay et al. (2011) determined the oblateness ratio of pumice grains in highly welded Bitlis ignimbrites (Turkey) between 0.07 and 0.20. Grain/matrix ratio (GMR) was calculated considering phenocryst, microlite, volcanic glass, void and opaque mineral ratio after point counting on thin sections under polarizing microscope by Korkanç and Solak (2016) as a petrographic indicator to define mechanical properties of tuffs. A significant statistical relationship was determined between plagioclase, void ratio and GMR ratio and geomechanical properties of Kızılkaya tuffs from Turkey. Eventually, high fenocrystal

rate and welding degree are associated with better mechanical properties.

A recent welding intensity classification comprising of six welding grades: grade I (nonwelded); grade II (sintered); grade III (very poorly welded); grade IV (moderately poorly welded); grade V (moderately densely welded) and grade VI (densely welded) for Ahlat ignimbrites was developed by Selçuk and Beyaz (2021). It is stated that dry unit weight, porosity, water absorption, abrasion and rock strength parameters are effective for the estimation of the degree of welding in ignimbrites (Fig. 5).

There are numerous scientific studies in the literature to reveal the engineering properties of ignimbrites. On the other hand, a few classifications have been developed to reveal the degree of welding of ignimbrites (Quane and Russell 2005a; Selçuk and Beyaz 2021). However, there are some limitations in these classifications and due to the simultaneous evaluation of many parameters, different parameter values may indicate different degrees of welding. In this study, a simple and practical two-parameter (uniaxial compressive strength and dry unit weight) welding degree classification for ignimbrites is proposed. In addition, the

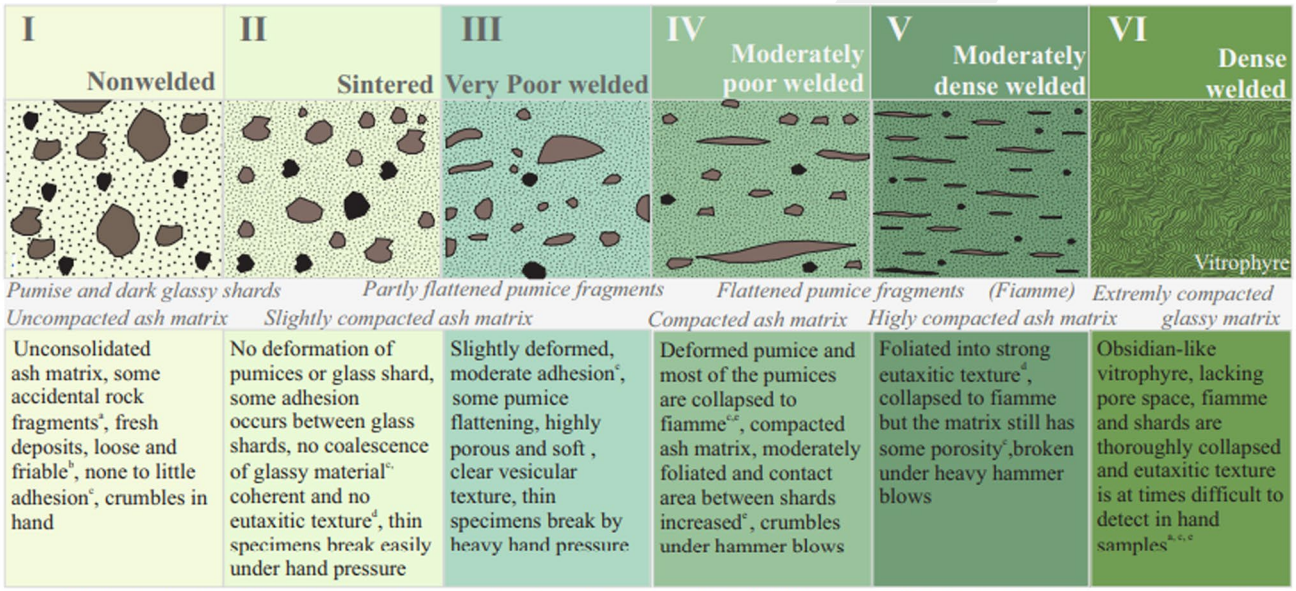

a) Smith (1960), b) Sheridan and Ragan (1976), c) Streck and Grunder (1995),d) Wilson and Hildreth (2003), e) Quane and Russell 2005.

Welding grade	Welding description	Dry unit weight kN/m^3	Porosity %	Water absorption %	Surface abrasion cm^3/50cm^2	P-wave velocity ms^{-1}	NPT mm	σ_c MPa	σ_t MPa	Strength description
VI	Densely welded	>23.0	<3.5	<1.0	<15.0	>3000	<6.0	>50.0	>4.0	High strength
V	Moderately Dense welded	16.5-23.0	25.0-3.5	[d]1.0-15.0	15.0-27.0	2400-3000	14.0-6.0	23.0-50.0	2.1-4.0	Medium strength
IV	Moderately poor welded	14.5-16.5	32.0-25.0	15.0-22.0	27.0-30.0	2000-2400	20.0-14.0	13.0-23.0	1.4-2.1	Low strength
III	Very poor welded	12.0-14.5	41.0-32.0	22.0-32.0	30.0-36.0	1750-2000	25.0-20.0	8.0-13.0	1.1-1.4	
II	Sintered	10.1-12.0	47.0-41.0	38.0-32.0	36.0-39.0	1400-1750	35.0-25.0	4.0-8.0	0.8-1.1	Very low strength
I	Nonwelded	<11.1	>43.0	>38.0	>37.0	<1500	Not applicable	<5.0	<0.8	

Fig. 5 Welding intensity classification of the Ahlat ignimbrites proposed by Selçuk and Beyaz (2021)

oblateness ratio of the pumice grains, which vary in proportion to the degree of welding in ignimbrites, are also evaluated in this study and accordingly welding degree classes are proposed.

Experimental studies

Ignimbrites, a pyroclastic rock type, may contain different amounts of lithic material and pumice as a consequence of their formation mechanism and may have varying degrees of welding due to pyroclastic flow temperatures. Therefore, it is quite probable to observe variations in physical and mechanical properties of ignimbrites. In order to provide sample diversity within the scope of this research study, ignimbrite samples were acquired from Central Anatolia (Kayseri and Nevşehir provinces) and Eastern Anatolia (Ahlat/Bitlis province) in Turkey, and experimental studies were carried out on these specimens. In the experimental studies, besides the cylindrical samples obtained from the block samples collected from the field, 7×7×7 cm cube samples cut in the quarries were also employed. On the other hand, in order to expand the data set, the results of several scientific studies performed on Nevşehir and Kayseri ignimbrites were also included in the study particularly during the development of welding classification.

Accordingly, a total of 16 different ignimbrite types (6 from Kayseri region, 7 from Nevşehir region and 3 from Ahlat region) with different textural, physical, chemical and mechanical properties were evaluated in this research. The sample codes and sampling locations of the ignimbrite samples used in the study are shown in Table 2. Additionally, close-up views of those specimens are depicted in Fig. 6.

Dry and saturated unit weight, water absorption by mass, apparent (effective) porosity, P-wave velocity in dry and saturated conditions and uniaxial compressive strength in dry and saturated conditions were determined on a total of 137 specimens in laboratory with respect to the recommendations of ISRM (2007). Furthermore, macro-scale shape factors of pumice fragments inside the ignimbrite samples were determined by means of microscopic measurements performed by an overhead illuminated microscope, and microscope images were transferred to NIS ELEMENTS (NIKON) software. Then, longitudinal (a) and axial (b) length of pumice were measured on a couple of surfaces of the ignimbrite sample in the same software (Fig. 7). Accordingly, the axial ratio (a/b), aspect ratio (b/a) and oblateness ratio (OR) (1-b/a) of each fragment were identified.

Whole-rock geochemistry analyses of 28 ignimbrite specimens were executed in ACME (Canada) analytical laboratories. Besides, major oxide element analyses used for classification of volcanic rocks were performed using ICP-ES (Inductively Coupled Plasma Emission Spectrometry) method.

Table 2 Sampling locations and sample codes and colors of the ignimbrites employed in the experimental studies

Sampling location		Sample code	Color
Province	Location		
Kayseri	Tomarza	Sh	Black
Kayseri	Tomarza	Kh	Brown
Kayseri	Tomarza	Kr	Reddish
Kayseri	Pınarbaşı	S	Yellow
Kayseri	Turan	G	Gray
Kayseri	Pınarbaşı	B	Beige
Nevşehir	Avanos	SB	Brownish
Nevşehir	Avanos	GK	Rose
Nevşehir	Ortahisar	OH	White
Nevşehir	Kavak	KV	White
Nevşehir	Demirtaş	DT	Gray
Nevşehir	Avanos	BJ	Beige
Nevşehir	Başdere	BD	Gray
Bitlis	Ahlat	N-1	Brown
Bitlis	Ahlat	N-2	Dark Brown
Bitlis	Ahlat	N-3-4	Light Brown

Electron probe microanalysis (EPMA) to determine the chemical compositions of some minerals (feldspar, biotite, amphibole and pyroxene) in the crystal components of 6 specimens were carried out at Ankara University Earth Sciences Application and Research Center using the JXA-8230 model EPMA instrument. The device has a B(5)-U(92) element measurement range, 6 nm resolution and 40X – 300.000X magnification. Analyses were performed on one-sided polished and carbon-coated thin sections. After vacuuming, the device was calibrated and brought to working conditions. Measurements were made at an accelerating voltage of 15 kV, a current of 20 nA, and a diameter of 5 µm. As a standard for elemental analysis; Wollastonite for Si and Ca, albite for Na, orthoclase for K, Al_2O_3 for Al, MgO for Mg, MnO for Mn, TiO_2 for Ti and Cr_2O_3 for Cr were used. Consequently, crystallization temperatures of the ignimbrites were estimated using the mineral compositions of the selected ignimbrites.

Results

Mineralogical and petrographic properties of the ignimbrites

Mineralogical and petrographic characteristics of the studied ignimbrites are summarized in Table 3. Selected ignimbrite samples differ in their composition (phenocrystal, lithic and

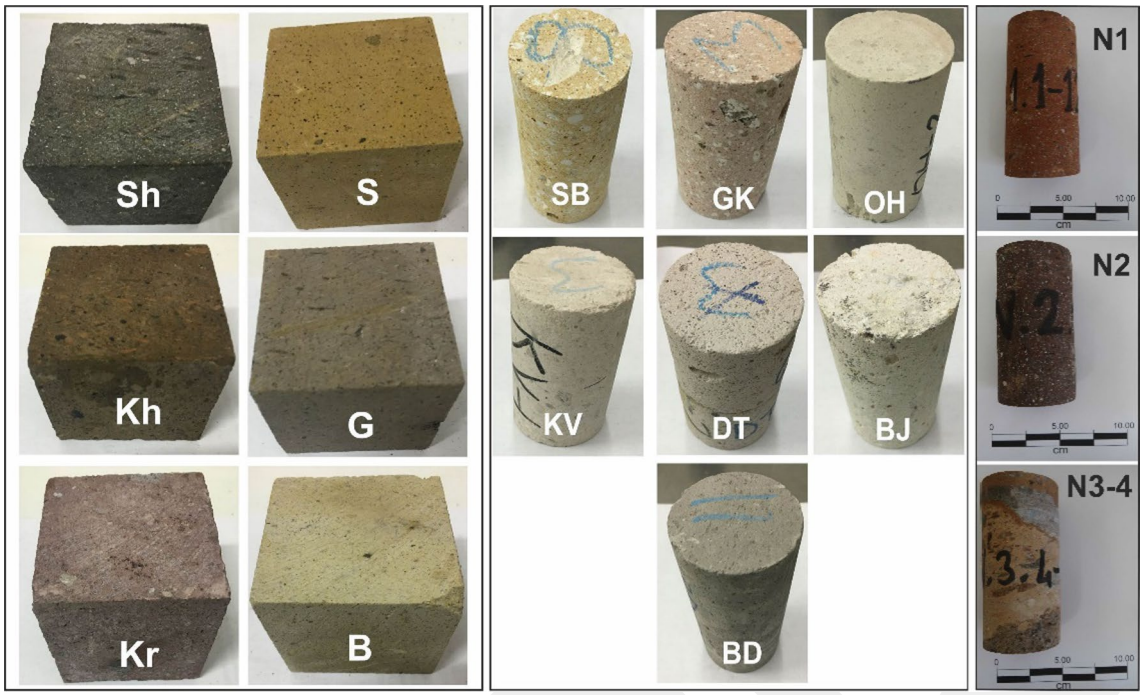

Fig. 6 Close-up views of the specimens investigated in this research

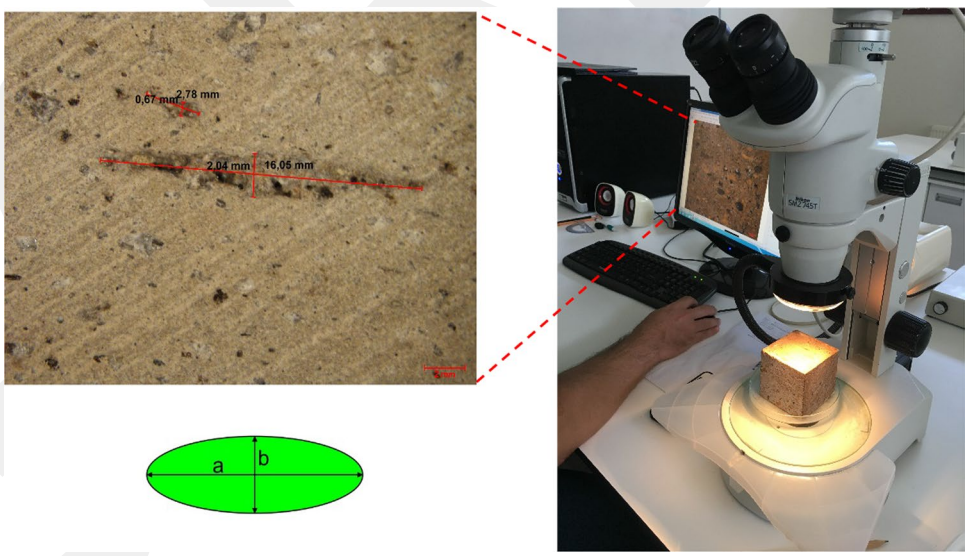

Fig. 7 Measurement of the longitudinal and axial length of pumice grains in the ignimbrites on the images captured by microscope

pumice fragments and volcanic glass) and their abundances. All ignimbrites have hypohyaline porphyritic texture. It contains volcanic glass shards and/or pumice fragments as a glass component.

Sh, Kh and Kr coded Tomarza ignimbrites reveal higher grain (phenocrystal and lithic) abundance than Pınarbaşı (S, B) and Turan (G) ignimbrites (Fig. 8). The ignimbrites in this region contain plagioclase, quartz, pyroxene, sanidine, feldspar and opaque minerals as phenocrysts. The lithic fragments are in hypocrystalline texture and probably in the composition of andesite and basalt (Fig. 8b, e). Plagioclases present as subhedral and prismatic crystals and generally polysynthetic twinning. Magma corrosion and sieve textures have developed in plagioclases. Similarly, gnawing is observed along the edges of quartz as a result of magma corrosion (Fig. 8 a, b). Less abundant pyroxenes are distinguished by their high interference colors. Elliptical and rounded-shaped pumice grains are observed. Pumices (Kh) in some samples present a flattened (fiamme) structure (Fig. 8c). Two

Table 3 Mineralogical and petrographic properties of the investigated ignimbrites

Location		Sample	Composition	Explanation
Kayseri	Tomarza	Sh	Phenocrystal (plg, q, prx, fld, op) + lithic and pumice fragments + volcanic glass	Grain (~ 30%) < volcanic glass (volcanic glass shards + pumice). Vitric tuff. Volcanic glass is observed as surrounding phenocrystal, lithic and pumice fragments. It presents eutaxitic texture
		Kh	Phenocrystal (plg, q, prx, fld, op) + lithic and pumice fragments + volcanic glass	Grain (~ 30%) < volcanic glass (volcanic glass shards + pumice). Vitric tuff. Vitrophiric texture is observed
		Kr	Phenocrystal (plg, prx, fld, op) + lithic fragments + volcanic glass	Grain (~ 50%) ≥ volcanic glass. Lithic fragment ratio is high. Lithic tuff. Vitrophiric texture is observed
	Pınarbaşı	S	Phenocrystal (plg, sn, op) + lithic fragments + volcanic glass	Grain < volcanic glass shards. Vitric tuff. Eutaxitic texture is observed
		B	Phenocrystal (plg, q, prx, fld, op) + lithic and pumice fragments + volcanic glass	Grain < volcanic glass shards + pumice. Vitric tuff. Eutaxitic texture is observed
	Turan	G	Phenocrystal (plg, q, prx, op) + volcanic glass	Grain < volcanic glass shards. Vitric tuff. Vitrophyric texture is observed
Nevşehir	Kavak	SB-2, 3	Phenocrystal (q, bio, op) + pumice fragments + volcanic glass	Grain (~ 5%) < volcanic glass + pumice. Pumice ratio is high. Vitric tuff. Vitrophyric texture is observed
		GK-1, 2, 3	Phenocrystal (q, bio, op) + pumice fragments + volcanic glass	Grain (~ 5%) < volcanic glass + pumice. Pumice ratio is high. Vitric tuff. Vitrophyric texture is observed
		BJ-1, 3, 5	Phenocrystal (q, plg, bio, op) + pumice fragments + volcanic glass	Grain (~ 5%) < volcanic glass + pumice. Pumice ratio is high. Vitric tuff. Vitrophyric texture is observed
		OH-1, 2	Phenocrystal (plg, q) + pumice fragments + volcanic glass	Grain (~ 5%) < volcanic glass + pumice. Pumice ratio is high. Vitric tuff. Vitrophyric texture is observed
		KV-1, 2, 3	Phenocrystal (plg, q, bio) + lithic and pumice fragments + volcanic glass	Grain (phenocrystal + lithic fragments ~ 15%) < volcanic glass shards. Vitric tuff. Gas bubbles in volcanic glass shards. Eutaxitic texture is observed
	Damsa	DT-1, 2	Phenocrystal (plg, q, bio, prx, fld, op) + lithic and pumice fragments + volcanic glass	Grain (~ 10%) < volcanic glass shards + pumice. Vitric tuff. Eutaxitic texture is observed
	Kızılkaya	BD-1	Phenocrystal (plg, q, bio, op) + lithic and pumice fragments + volcanic glass	Grain (~ 5%) < volcanic glass + pumice. Vitric tuff. Eutaxitic texture is observed
Bitlis	Ahlat	N-1, N-2, N-3–4	Phenocrystal (plg, sn, q, amf, prx, op) lithic and pumice fragments + volcanic glass	Grain (~ 15%) < volcanic glass shards + pumice. Vitric tuff. Eutaxitic texture (N-1, N-2) and vitrophyric texture (N-3) are observed

types of pumice were distinguished in the ignimbrites of Kayseri region. These are pumices with (Sh, Kh) and without (B) phenocrysts (Fig. 8b, c and h). Pumice with phenocryst contains plagioclase, pyroxene and opaque minerals. Its matrix is crystalline quartz. Some samples contain large-surfaced V–Y shaped volcanic glass shards (Fig. 8f–i). Volcanic glass shards are located surrounding phenocryst, lithic and pumice clasts. In some samples (Sh, S and B), the grains depict orientation within the volcanic glass shards and typical eutaxitic textures have developed (Fig. 8). According to the classification of Schmid (1981), the Sh, Kh, S, B and G samples of the Kayseri Region were classified as vitric tuff and the Kr sample as lithic tuff (Table 3).

Pumice abundance in the Nevşehir ignimbrites (SB, G, BJ and OH samples) is considerably higher than Damsa and Kızılkaya ignimbrites (Table 3 and Fig. 9a–d). The ignimbrites in the region contain plagioclase, quartz, biotite, pyroxene and opaque minerals as phenocrysts. Lithic fragments are in hypocrystalline texture and probably in basalt composition (Fig. 9e, i). Plagioclases usually present prismatic crystals and polysynthetic twinning (Fig. 9f). Magma corrosion textures were observed in plagioclase and quartz (Fig. 9h–i). Biotite is characteristic with brown and elongated plate-like shape (Fig. 9f–h). Opacifications are observed along the edges. Pumice grains do not present fiamme structures indicating low welding intensity. While pumice edges are prominent in samples containing

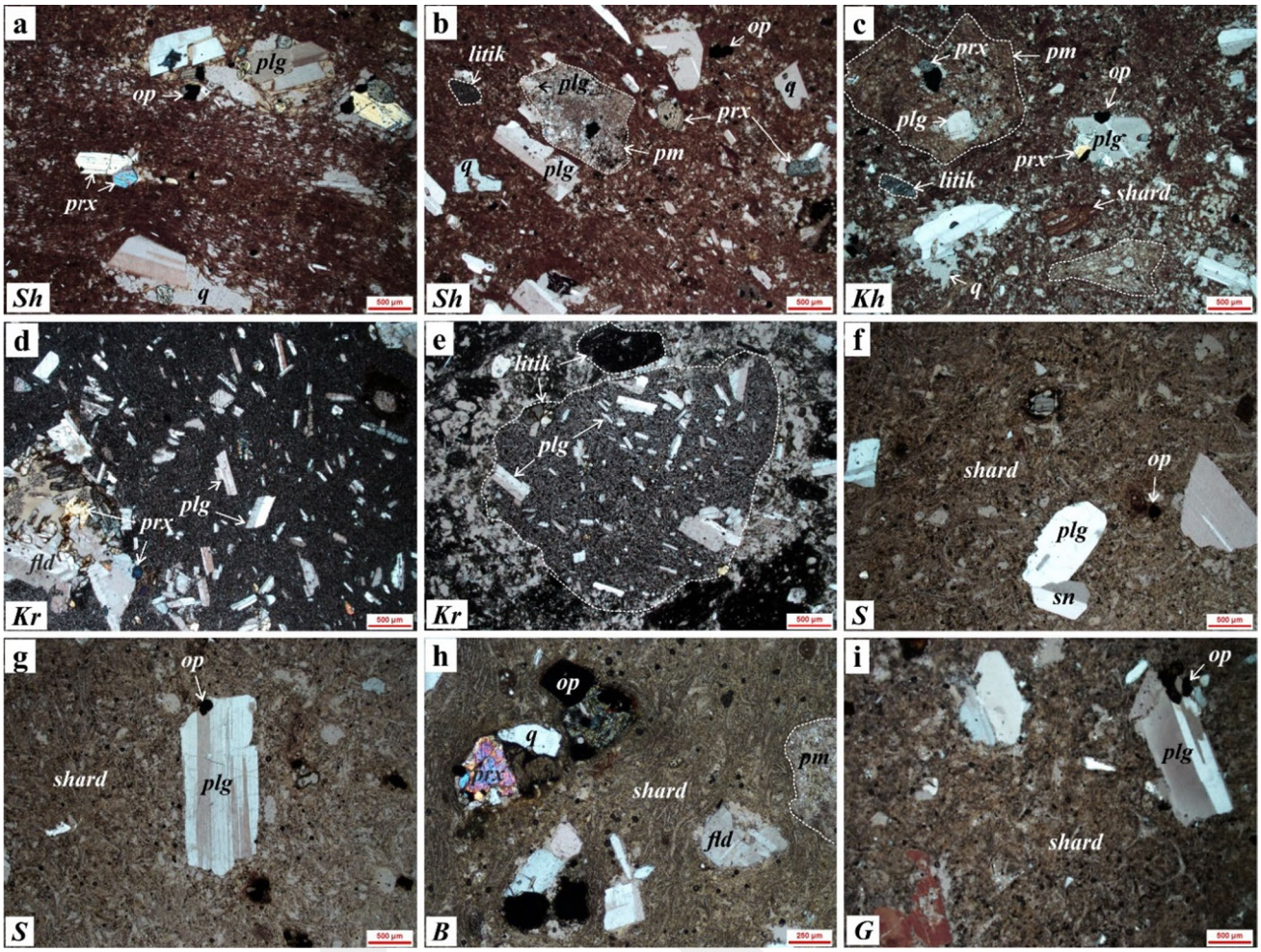

Fig. 8 Kayseri-Tomarza (Sh, Kh, Kr), Pınarbaşı (S, B) and Turan (G) ignimbrites; **a**, **b** Eutaxitic texture in sample Sh; **c** pumice and lithic fragments containing phenocryst and phenocryst in sample Kh; **d**, **e** the Kr sample rich in phenocryst and rock fragments; **f**, **g** In sample S; **h** in and in sample B, typical eutaxitic texture with abundant volcanic glass shards; **i** double nicol microscopy images of vitrophyric texture with abundant volcanic glass shards in sample G. *fld* feldspar, *lithic* rock fragment, *op* opaque, *plg* plagioclase, *pm* pumice, *prx* pyroxene, *shard* volcanic glass shards, *sn* sanidine, *q* quartz

phenocrystal (biotite, quartz) pumice (KV, DT), the contacts are indistinct and transitive in samples containing pumice without phenocrystal (SB, GK, BJ, OH) (Fig. 9a–g). In some samples (KV, DT, BD), large-surfaced V–Y shaped volcanic glass shards surround the phenocryst, lithic and pumice fragments (Fig. 9e–i). Gas cavities are observed within volcanic glass shards in KV specimens where eutaxitic texture develop (Fig. 9e). According to the classification of Schmid (1981), all ignimbrite samples of Nevşehir region (SB, GK, BJ, OK, KV, DT and BD) are classified as vitric tuff (Table 3).

The grain abundance (phenocrystal + lithic fragment) of the Ahlat ignimbrites (N-1, N-2, N-3-4) in the Bitlis Region is around 15%. It contains plagioclase, sanidine, quartz, amphibole, pyroxene and opaque minerals as phenocrysts (Table 3 and Fig. 10). Lithic fragments are probably in obsidian, trachyte composition. Plagioclases generally present prismatic crystals and polysynthetic twinning (Fig. 10). Plagioclase and quartz present magma corrosion textures. Volcanic glass shards and pumice are observed as volcanic glass. It is observed that the phenocrystal, lithic and pumice fragments of the volcanic glass shards are completely surrounded revealing an eutaxitic texture. Pumice grains typically present fiamme structures (Fig. 10a). The Ahlat ignimbrites are classified as vitric tuff with respect to the classification of Schmid (1981).

Geochemical classification of the ignimbrites

Whole rock geochemical composition of the selected ignimbrites is presented in Table 4. Except the ignimbrites of Nevşehir region (SB, GK, BJ, OH, KV), it was determined

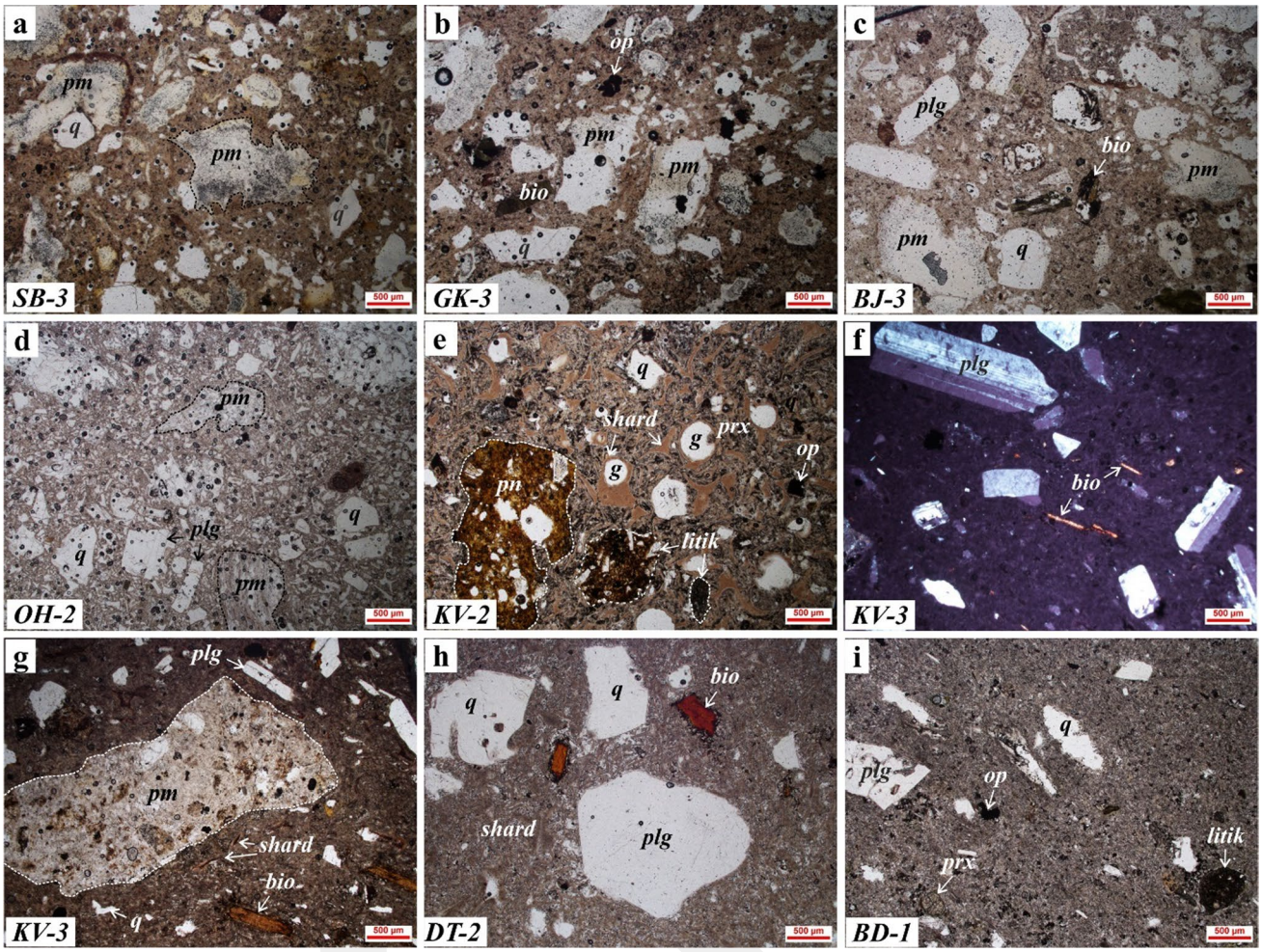

Fig. 9 Nevşehir-Kavak (SB, GK, BJ, OH, KV), Damsa (DT) and Kızılkaya (BD) ignimbrites; **a** SB; **b** GK-3; **c** BJ-3 and **d** OH-2 samples have vitrophyric texture with abundant pumice fragments; **e** gas cavities in phenocryst, pumice and lithic fragments and volcanic glass shards in sample KV-2, **f**, **g** phenocrysts and pumice fragments in volcanic glass shards in sample KV-3; **h** phenocrystal and glass shards in sample DT; **i** eutaxitic texture in sample BD-1 (*bio* biotite, *fld* feldspar, *g* gas cavities, *lithic* rock fragment, *op* opaque, *plg* plagioclase, *pm* pumice, *prx* pyroxene, *shard* volcanic glass shards, *q* quartz) (***a***–***e*** single nicol, ***f*** double nicol)

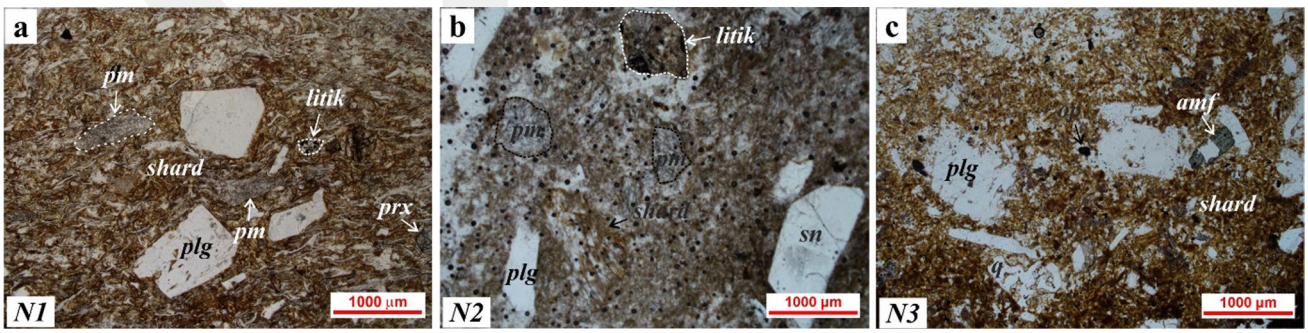

Fig. 10 The Ahlat (Bitlis) ignimbrites; **a**, **b** Single-nicol microscope images of volcanic glass shards and eutaxitic texture in samples N-1 and N-2 and vitrophyric texture in samples **b** N-2 and **c** N-3 (*amp* amphibole, *lithic* rock fragments, *op* opaque, *plg* plagioclase, *pm* pumice, *prx* pyroxene, *shard* volcanic glass shards, *sn* sanidine, *q* quartz)

Table 4 Geochemical composition of studied ignimbrites

Location	Tomarza			Pınarbaşı		Turan	Kavak												
Sample code	Sh	Kh	Kr	S	B	G	SB-2	SB-3	GK-1	GK-2	GK-3	BJ-1	BJ-3	BJ-5	OH-1	OH-2	KV-1	KV-2	KV-3
Major oxide (%)																			
SiO_2	64.96	63.52	61.33	72.69	68.25	71.92	77.93	78.64	76.86	76.85	76.32	79.08	78.94	78.54	68.97	75.04	66.81	69.66	73.09
Al_2O_3	15.26	15.5	16.34	14.05	14.3	14.49	13.57	13.51	14.23	14.25	14.16	13.46	13.64	13.88	13.51	11.39	14.12	14.01	13.62
Fe_2O_3	4.23	4.45	6.31	1.73	4.05	2.16	1.26	1.05	1.58	1.56	1.59	0.61	0.7	0.55	1.46	1.04	1.34	2.08	1.79
MgO	1.0	1.17	2.08	0.22	0.58	0.39	0.08	0.08	0.21	0.22	0.22	0.12	0.11	0.12	0.93	0.13	1.2	0.72	0.34
CaO	2.78	3.3	4.84	0.94	1.79	1.31	0.1	0.09	0.13	0.12	0.54	0.09	0.08	0.09	1.29	1.41	1.56	1.42	1.31
Na_2O	4.42	4.56	4.56	4.69	4.4	4.87	0.07	0.07	0.07	0.07	0.07	0.07	0.07	0.07	1.22	1.91	1.44	2.81	3.85
K_2O	3.11	2.97	2.03	4.26	3.74	3.99	0.32	0.31	0.54	0.50	0.59	0.40	0.38	0.38	3.61	3.86	3.66	4.73	4.28
TiO_2	0.77	0.81	1.12	0.35	0.54	0.4	0.19	0.18	0.19	0.19	0.19	0.19	0.19	0.18	0.15	0.14	0.16	0.29	0.27
P_2O_5	0.16	0.18	0.26	0.04	0.1	0.06	0.05	0.04	0.04	0.04	0.04	0.04	0.03	0.03	0.02	0.01	0.04	0.07	0.06
MnO	0.08	0.09	0.1	0.04	0.06	0.07	< 0.01	< 0.01	0.07	0.02	0.06	< 0.01	< 0.01	< 0.01	0.07	0.05	0.14	0.07	0.07
Cr_2O_3	< 0.002	< 0.002	0.003	< 0.002	0.01	< 0.002	< 0.002	< 0.002	< 0.002	< 0.002	< 0.002	0.002	< 0.002	< 0.002	< 0.002	< 0.002	< 0.002	< 0.002	< 0.002
LOI	3.0	3.3	0.8	0.8	2.0	0.2	6.3	5.9	5.9	6.1	6.1	5.8	5.8	6	8.6	4.9	9.3	3.9	1.1
Total	99.96	99.95	99.94	99.98	99.97	99.98	99.87	99.87	99.82	99.92	99.88	99.86	99.94	99.84	99.83	99.88	99.77	99.76	99.78

Location	Damsa		Kızılkaya	Ahlat		
Sample code	DT-1	DT-2	BD-1	N-1	N-2	N-3-4
Major oxide (%)						
SiO_2	67.00	73.93	68.13	66.25	66.80	72.43
Al_2O_3	14.97	13.31	14.23	16.03	15.53	12.44
Fe_2O_3	4.89	2.26	4.02	4.47	4.49	4.28
MgO	1.11	0.4	0.47	0.21	0.20	0.04
CaO	2.6	1.52	2.35	1.45	1.46	0.45
Na_2O	4.55	3.66	4.61	5.90	5.85	4.96
K_2O	3.37	4.08	3.9	5.11	5.11	5.10
TiO_2	0.65	0.24	0.51	0.40	0.38	0.26
P_2O_5	0.15	0.05	0.12	0.06	0.07	0.01
MnO	0.08	0.06	0.05	0.14	0.14	0.11
Cr_2O_3	0.002	< 0.002	< 0.002			
LOI	0.4	0.3	1.4			
Total	99.77	99.81	99.79	100.0	100.0	100.0

by mineralogical-petrographic analysis that the ignimbrite samples contain substantial number of lithic fragments. In the total alkali (Na_2O+K_2O) vs. SiO_2 diagram (Middlemost 1994), Kayseri ignimbrites are identified as andesite (Kr), trachydacite (S, Kh and B) and rhyolite (S and G) (Fig. 11). The Ahlat (Bitlis) ignimbrites are in the composition of trachyandesite (N-1 and N-2) and rhyolite (N-3–4). The Nevşehir ignimbrites, on the other hand, exhibit varying compositions (Fig. 11). The Kavak ignimbrite is in dacite and trachydacite (KV) and rhyolite (OH) composition. The majority of the Kavak ignimbrite with abundant pumice grains are pinned on dacite-rhyolite-silexite (SB, Gk and BJ) areas. Damsa (DT) and Kızılkaya (BD) samples have trachydacite and rhyolite compositions.

EPMA mineral chemistry analyzes of phenocrysts were carried out on a limited number of specimens from each region (Sh: Tomarza/Kayseri; BJ1: Kavak/Nevşehir; N-3–4: Ahlat/Bitlis) to estimate the crystallization temperature (T) of ignimbrites. The EPMA analyses were performed on the plagioclase, pyroxene and hornblende minerals of Sh (Tomarza), on the pyroxene and hornblende minerals of N-3–4 (Ahlat) and on the biotite mineral of BJ1 (Kavak) coded specimens, and the results are presented in Table 5.

The plagioclase minerals of the Tomarza and Ahlat ignimbrites are in andesine (Ab_{54-65}) composition (Fig. 12a) whereas pyroxene is in augite (Fig. 12b). Hornblendes are in magnesio-hornblende (Fig. 12c). Moreover, the biotites of the Kavak ignimbrite are composed of Mg-biotite (Fig. 12d). Temperatures of plagioclases from the Tomarza ignimbrite was determined from the liquid-plagioclase geothermometric spreadsheet provided by Putirka (2008). To calculate the temperatures of hornblendes in the Tomarza and Ahlat ignimbrites, the thermobarometric formulation developed by Ridolfi (2021) for calc-alkaline and alkaline magma and calcic amphiboles in equilibrium was used. Besides, the crystallization temperatures of biotite were determined on the basis of Luhr et al. (1984). The temperature curves of Lindsley and Anderson (1983) were employed to estimate the pyroxene crystallization temperatures (Fig. 12b). Estimated crystallization temperatures of the ignimbrites using mineral compositions are depicted in Table 6. The highest formation temperature values ranging from 726 to 1100 ℃ were obtained in the Tomarza (Kayseri) ignimbrites with trachydacite composition and eutaxitic textures. The crystallization temperature values of the Ahlat ignimbrites with rhyolite composition vary between 600 and 854 ℃. The temperature values of the Kavak (Nevşehir) ignimbrites with silexite composition and high pumice component are between 688 and 710 ℃.

Physical and mechanical properties of the ignimbrites

Some experimental studies were executed to determine the physical and mechanical properties of the ignimbrite samples with different color and texture properties. Consequently, dry and saturated unit weight, water absorption and apparent porosity of the ignimbrites were revealed. On the other hand, P-wave velocity measurements and uniaxial compressive strength (UCS) tests were performed for dry and saturated conditions as well. It should be noted that as several ignimbrite specimens exhibit anisotropy with respect to the depositional characteristics and welding, the ultrasonic velocity tests were performed parallel to the fiamme

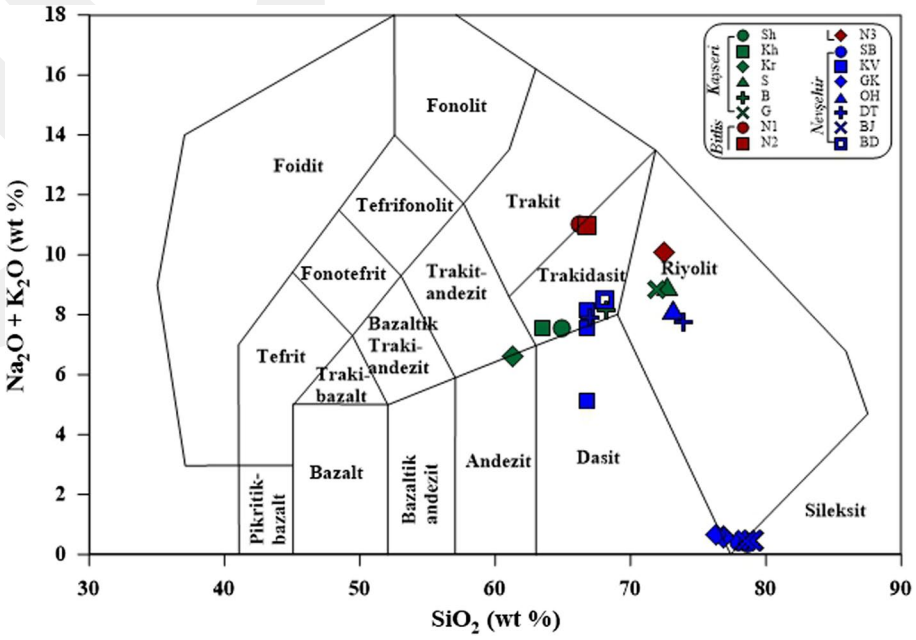

Fig. 11 Classification of the studied ignimbrites based on the diagram of total alkali (Na_2O+K_2O) versus SiO_2 (Middlemost 1994)

Table 5 Representative EPMA results of plagioclase, pyroxene, hornblende and biotite for the Tomarza (Kayseri), Kavak (Nevşehir) and Ahlat (Bitlis) ignimbrites

Location	Tomarza (Kayseri)									Kavak (Nevşehir)			Ahlat (Bitlis)					
Minerals	Plagioclase ($n=9$)			Pyroxene ($n=7$)			Hornblende ($n=7$)			Biotite ($n=6$)			Pyroxene ($n=4$)			Hornblende ($n=6$)		
	Min	Max	Mean	Min	Max	Mean	Min	Max	Mean	Min	Max	Mean	Min	Max	Mean	Min	Max	Mean
SiO_2	46.88	55.83	50.99	43.14	44.61	44.17	41.93	46.72	45.77	34.89	35.61	35.17	44.00	45.86	44.93	45.49	47.92	47.92
TiO_2	0.03	0.06	0.06	0.42	0.46	0.45	0.41	0.71	0.56	4.18	4.47	4.41	0.39	0.63	0.51	0.75	0.89	0.82
Al_2O_3	27.25	34.91	32.56	2.19	5.73	2.86	8.17	14.04	8.81	13.41	14.53	13.90	1.23	1.69	1.77	7.02	7.17	7.17
FeO	0.48	0.58	0.52	25.69	27.09	26.78	11.49	13.65	12.39	22.14	23.21	22.18	20.87	22.53	21.70	14.49	15.93	15.05
MnO	0.00	0.00	0.00	0.88	0.98	0.91	0.33	0.50	0.34	0.13	0.25	0.19	0.22	0.27	0.23	0.65	1.03	0.91
MgO	0.00	0.03	0.00	4.51	5.71	4.99	12.55	13.94	13.43	10.68	11.34	11.28	11.28	12.22	11.75	13.70	18.16	14.48
CaO	7.50	10.23	9.24	18.33	19.67	19.36	14.46	17.46	15.43	0.03	0.28	0.17	16.83	20.13	18.44	8.40	10.14	9.41
Na_2O	5.64	8.26	6.37	0.22	0.32	0.26	0.20	1.21	0.76	0.20	0.23	0.22	0.19	0.24	0.21	1.22	1.55	1.17
K_2O	0.19	0.45	0.36	0.00	0.06	0.00	0.00	0.03	0.01	7.19	9.40	7.89	0.00	0.00	0.00	0.27	0.53	0.32
Total	99.39	100.89	100.11	99.07	100.24	99.78	99.24	100.84	99.54	94.09	97.68	95.49	99.20	100.54	99.54	99.13	99.73	99.37
Si	2.160	2.533	2.310	1.712	1.789	1.772	6.229	6.873	6.820	5.385	5.454	5.430	1.707	1.768	1.738	6.275	6.867	6.778
Ti	0.001	0.002	0.002	0.013	0.014	0.014	0.000	0.000	0.000	0.480	0.526	0.512	0.011	0.019	0.015	0.000	0.560	0.053
Al^{IV}	1.895	1.457	1.743	0.103	0.268	0.135	1.127	1.771	1.180	2.471	2.614	2.528	0.055	0.089	0.081	1.133	1.179	1.169
Al^{VI}	–	–	–	–	–	–	0.071	0.646	0.282	0.000	0.016	0.000	–	–	–	0.000	0.052	0.026
Fe^{2+}	0.018	0.022	0.020	0.597	0.809	0.770	2.780	3.054	2.983	2.834	2.964	2.864	0.611	0.660	0.635	2.928	3.735	3.050
Fe^{3+}				0.093	0.263	0.128	0.000	0.014	0.007	–	–	–	0.041	0.066	0.066	1.395	3.155	1.840
Mn	0.000	0.000	0.000	0.030	0.033	0.031	0.041	0.064	0.043	0.017	0.033	0.024	0.007	0.009	0.008	0.076	0.124	0.109
Mg	0.000	0.002	0.000	0.270	0.327	0.298	2.780	3.054	2.983	2.430	2.572	2.597	0.653	0.702	0.677	2.928	3.934	3.128
Ca	0.362	0.497	0.450	0.791	0.847	0.832	2.280	2.806	2.466	0.005	0.046	0.028	0.695	0.834	0.764	1.307	1.557	1.459
Na	0.496	0.724	0.562	0.017	0.024	0.020	0.057	0.353	0.222	0.060	0.068	0.066	0.014	0.018	0.016	0.321	0.438	0.330
K	0.011	0.026	0.021	0.000	0.003	0.000	0.000	0.006	0.003	1.433	1.822	1.552	0.000	0.000	0.000	0.049	0.099	0.060
Or	1.08	2.32	2.00															
Ab	49.40	64.52	54.36															
An	33.59	49.52	43.65															
Wo				38.17	40.72	40.47							32.70	38.63	35.67			
En				13.38	15.62	14.49							30.18	33.05	31.64			
Fs				43.20	44.94	44.07							30.47	33.45	31.96			

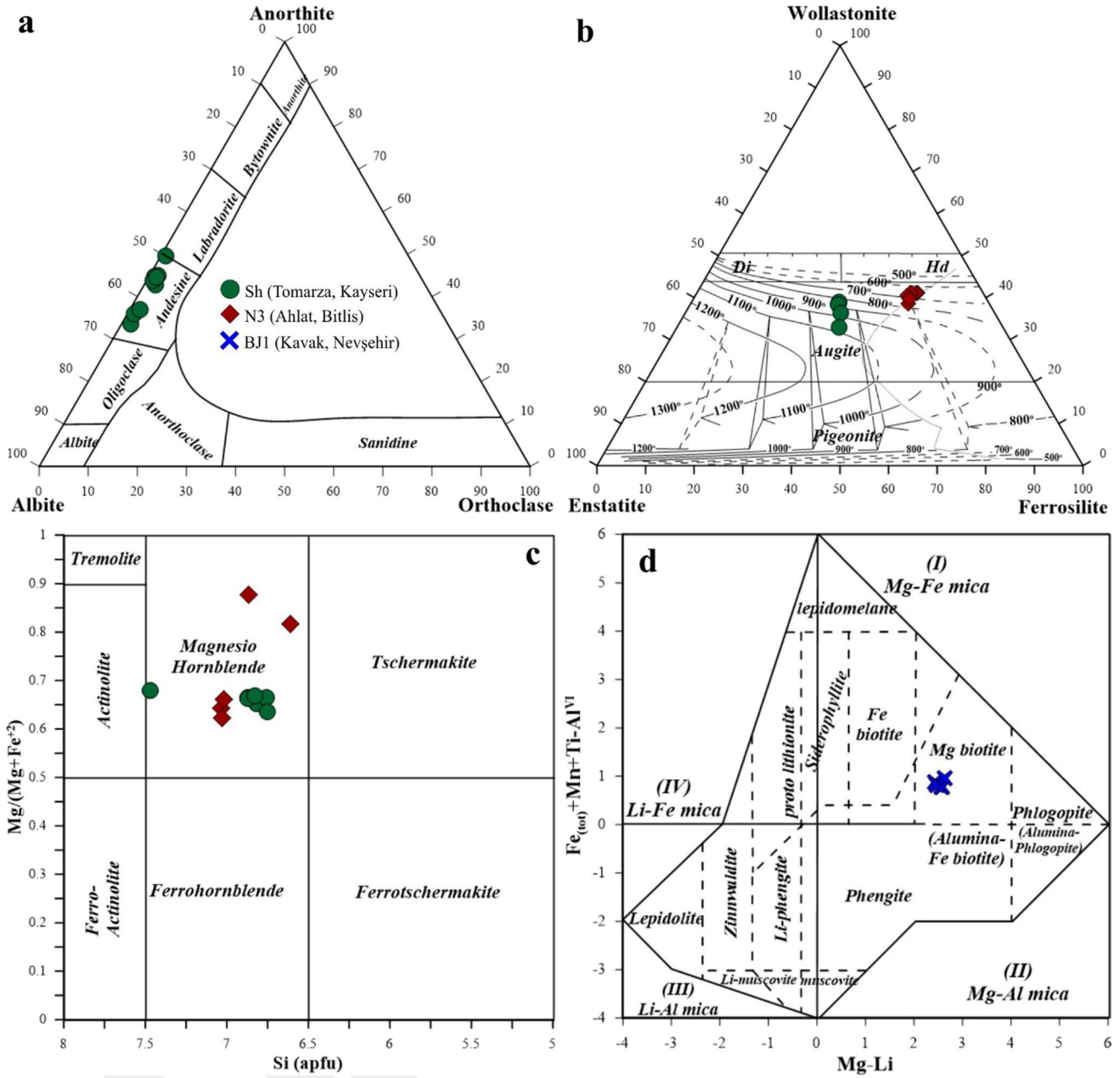

Fig.12 Classification of **a** feldspar on the An–Ab–Or ternary diagram (Deer et al. 1992); **b** pyroxenes on the Wo–En–Fs ternary diagram (Morimoto, 1988) (temperature curves are taken from Lindsley and Andersen 1983); **c** amphiboles on the Si versus Mg# (apfu) (Leake et al. 1997) **d** biotite on the trioctahedral micas (Tischendorf et al. 1997)

Table 6 Estimated crystallization temperatures considering different minerals for the Tomarza (Kayseri), Kavak (Nevşehir) and Ahlat (Bitlis) ignimbrites

Region	Tomarza (Kayseri)	Kavak (Nevşehir)	Ahlat (Bitlis)	References
Rock	Trachydacide	Silexite	Rhyolite	
Texture	Eutaxitic	Vitrophyric	Eutaxitic	
Pyroxene	800–1100 ℃		600–800 ℃	Lindsley and Anderson (1983)
Amphibole	726–819 ℃		851–854 ℃	Ridolfi (2021)
Biotite		688–710 ℃		Luhr et al. (1984)
Plagioclase	940–962 ℃			Putirka (2008)

structures whereas specimens were loaded normal to those structures during uniaxial compressive strength tests. Average values of physico-mechanical properties of the different ignimbrite samples are presented in Table 7.

As presented in Table 7, the average dry unit weight values of selected ignimbrites vary between 13.45 and 17.84 kN/m^3. Hence, it is concluded that all ignimbrites of this study are classified as very low unit weight rocks in accordance with the ANON (1979) classification. As known, ignimbrite is a type of rock with a highwater absorption capacity. For this reason, there may be significant differences between dry and saturated unit weights of the ignimbrites. Dry and saturated unit weight values of the ignimbrites from Kayseri and Ahlat regions are close to each other whilst the difference is much noticeable for the Nevşehir specimens. Furthermore, the saturated unit weight of the studied ignimbrites can be as high as 19.73 kN/m^3.

As a result of laboratory experiments, it was determined that the ignimbrite samples present high water absorption and apparent porosity values, as expected. The apparent porosity values of the Kayseri and Ahlat ignimbrites vary between 15.99% and 27.96% as well as 20.35% and 28.89%, respectively. On the other hand, the apparent porosity of the Nevşehir ignimbrites may exceed 30%. Eventually, it is concluded that the Kayseri and Ahlat ignimbrites are highly porous according to the ANON (1979) classification, while the Nevşehir ignimbrites have very high porosity.

The average P-wave velocity of the Kayseri ignimbrites in dry conditions is around 2000 m/s and may attain a maximum velocity of 2700 m/s for Sh and Kh coded ignimbrites (Table 7). Dry P-wave velocity of the Nevşehir ignimbrites was determined to be below 2000 m/s. Moreover, average P-wave velocities in the Ahlat ignimbrites are between 1709 and 2623 m/s for dry samples. All ignimbrite samples with a P-wave velocity below 2500 m/s are classified as rocks with very low P-wave velocity (ANON 1979). Sh, Kh (Kayseri) and N-3–4 (Ahlat) coded ignimbrites with a P-wave velocity higher than 2500 m/s are in the low P-wave velocity rock class. Finally, is a decrease in the P-wave velocity under saturated conditions is remarkable for the Kayseri and Ahlat ignimbrites.

As a result of uniaxial compressive strength tests carried out in dry conditions to determine the strength of the ignimbrites, it was revealed that the uniaxial compressive strength (σ_c) of the Kayseri ignimbrites is generally above 20 MPa. A maximum and minimum of 36.84 MPa and 17.26 MPa were obtained for G and B-coded Kayseri ignimbrites, respectively. Accordingly, the Kayseri ignimbrites are classified as medium strength rocks according to the ANON (1979) classification. The Nevşehir ignimbrites have the lowest uniaxial compressive strength among the studied samples. An average uniaxial compressive strength of 10 MPa and even lower strength values were obtained for the tested specimens. While the average dry σ_c values of N-1 and N-2 coded Ahlat ignimbrites are around 15 and 12 MPa, the UCS of N-3–4 ignimbrites attains 30 MPa. Therefore, the Nevşehir and Ahlat ignimbrites are classified as weak strength rocks according to ANON

Table 7 Average physico–mechanical properties of the ignimbrites of Kayseri, Nevşehir and Ahlat regions

Location	Sample code	Dry unit weight (kN/m^3)	Saturated unit weight (kN/m^3)	Apparent porosity (%)	Water absorption by weight (%)	P–wave velocity–dry (m/s)	P–wave velocity–saturated (m/s)	Uniaxial compressive strength–dry (MPa)	Uniaxial compressive strength–saturated (MPa)
Kayseri	Sh	15.71	16.73	26.32	18.29	2785	2487	21.05	14.01
	Kh	14.64	16.73	26.94	18.76	2710	2694	22.52	16.8
	Kr	17.42	19.24	22.18	12.75	2090	1897	20.65	18.86
	S	15.37	18.3	28.72	18.19	2045	1896	20.92	16.18
	G	17.84	19.73	15.99	8.63	1965	1695	36.84	32.8
	B	15.78	18.53	27.96	17.37	1936	1748	17.26	15.65
Nevşehir	SB	14.08	17.04	28.22	29.68	1670	–	7.77	–
	GK	13.93	16.40	24.73	23.94	1642	–	11.78	–
	OH	13.71	–	24.80	18.90	2013	–	19.24	17.30
	KV	13.45	–	31.1	22.62	1759	–	11.3	6.3
	DT	15.00	–	32.41	21.33	1562	–	11.34	9.91
	BJ	13.86	17.29	36.67	33.8	692	–	6.64	–
	BD	14.44	–	35.12	24.11	1865	–	14.41	13.25
Ahlat	N-1	15.13	17.89	28.89	18.68	1709	1554	15.78	13.59
	N-2	15.77	18.60	27.40	16.92	2378	2257	12.10	12.17
	N-3–4	16.82	18.59	20.35	12.03	2623	2212	28.92	26.83

(1979), with the exception of the samples coded OH, N-1 and N-3–4.

The UCS under saturated conditions were also determined in some of the ignimbrite samples. In a number of samples of the Kayseri ignimbrites, a strength decrease of more than 30% under saturated conditions was determined. On the other hand, in the Nevşehir ignimbrites, the σ_c decreased significantly under saturated conditions, specifically for the KV-coded sample. On the contrary, there is no significant strength decrease under saturated conditions in the Ahlat ignimbrites. The test results indicate that some ignimbrites are very sensitive to surface water and may drastically lose their strength. As a summary, the bar diagrams of physical and mechanical properties of the selected ignimbrites are illustrated in Fig. 13.

Shape and dimension of pumice fragments in the studied ignimbrites

Long and short axis measurements of pumice grains in the ignimbrite samples obtained from Kayseri, Nevşehir and Ahlat regions were determined within the framework of the principles depicted in Fig. 7. In Table 8, for a number of 16 different ignimbrite types of Kayseri, Nevşehir and Ahlat regions, the lowest, highest and average long axis (a), short axis (b) lengths determined for the pumice grains and the axial ratio (a/b), aspect ratio (b/a) and oblateness ratio (OR) [1-(b/a)] values calculated according to these lengths are presented. On the other hand, bar graphs of different shape parameter (a/b, b/a, OR) values calculated for pumice grains in the ignimbrites are given in Fig. 14.

The axial ratio (a/b) value approaching 1 indicates that the axis lengths of the grain get closer to each other and therefore the grain shape reveals a more rounded structure. On the other hand, the range of aspect ratio (b/a) is between 0 and 1. While values approaching 1 point out that the material shape is closer to circle, the aspect ratio values around 0 represent lenticular grains due to the increase in long axis. For the oblateness ratio (OR), values around 0 mention that the shape of the examined material is round. Conversely, the material shape is more lenticular for values closer to 1.

Figure 14 depicts the column chart prepared according to the average shape parameters of the pumice grains in 16 different ignimbrite types. In this graph, it is noteworthy that there are significant variations in the shape parameters of the pumice grains among the ignimbrites. When the axial ratio (a/b) values of the ignimbrites obtained from the Kayseri region are examined, it is realized that the a/b ratio exceeds 5 especially in the Sh (black) and G (grey) coded samples indicating that the pumice grains in these ignimbrites are quite lenticular. The lowest axial ratio value among the Kayseri ignimbrites is associated with the Kr coded red ignimbrites with a value of 1.62. The distribution of aspect ratio (b/a) ratio in the Kayseri ignimbrites shows a similar trend to the axial ratio. The lowest aspect ratio was also determined for the Sh and

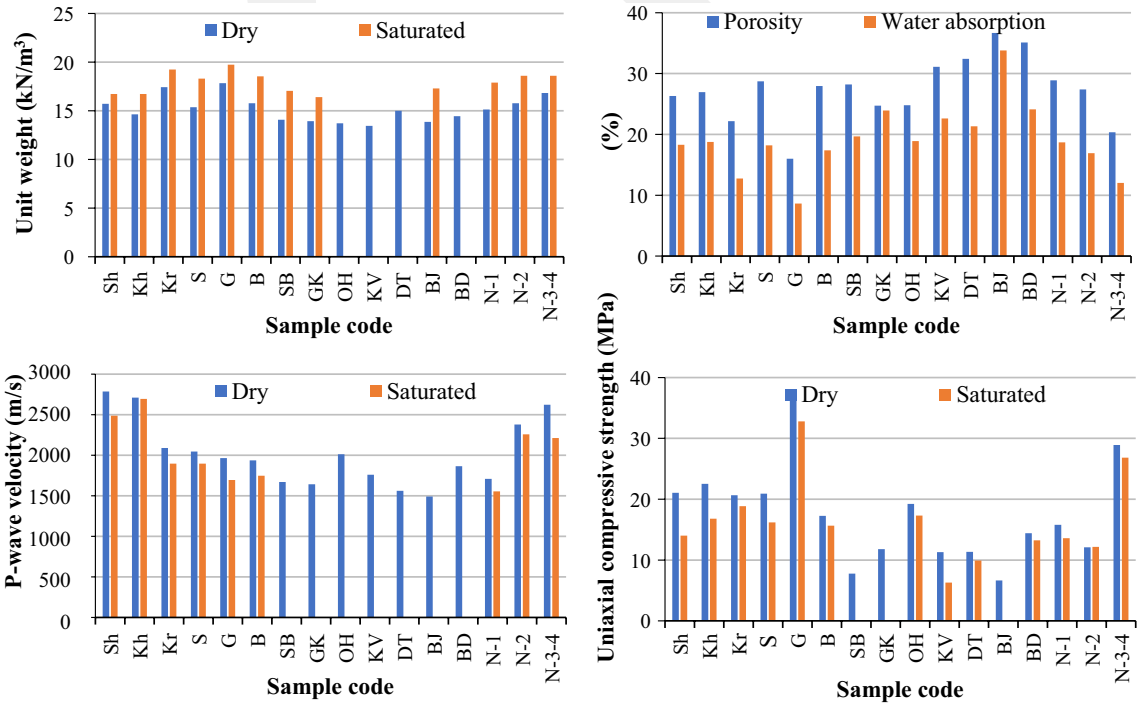

Fig. 13 Bar diagrams of physical and mechanical properties of the studied ignimbrites

Table 8 Axis lengths and different shape parameter values of pumice grains in the ignimbrites

Location	Sample code	Pumice				
		Long axis (mm) (a)	Short axis (mm) (b)	a/b	b/a	OR
KAYSERİ	Sh					
	Minimum	1.27	0.31	1.05	0.05	0.05
	Maximum	22.93	3.58	19.59	0.95	0.95
	Average	4.39	0.90	5.35	0.24	0.76
	Std. dev.	3.32	0.57	3.15	0.13	0.13
	Kh					
	Minimum	0.75	0.30	1.54	0.12	0.35
	Maximum	50.00	7.00	8.63	0.65	0.88
	Average	3.60	0.96	3.35	0.35	0.65
	Std. dev.	6.18	0.97	1.45	0.13	0.13
	Kr					
	Minimum	0.58	0.49	1.00	0.33	0.00
	Maximum	16.01	10.29	3.06	1.00	0.67
	Average	3.35	2.15	1.62	0.66	0.34
	Std. dev.	2.43	1.53	0.46	0.16	0.16
	S					
	Minimum	0.75	0.28	1.55	0.08	0.92
	Maximum	13.89	6.94	12.32	0.65	0.35
	Average	2.61	0.93	3.24	0.38	0.62
	Std. dev.	2.45	1.06	2.00	0.14	0.14
	G					
	Minimum	1.43	0.36	1.77	0.05	0.95
	Maximum	16.05	4.94	20.70	0.57	0.43
	Average	5.75	1.21	5.29	0.24	0.76
	Std. dev.	3.97	0.88	3.20	0.11	0.11
	B					
	Minimum	0.85	0.31	1.70	0.18	0.82
	Maximum	8.67	2.58	5.69	0.59	0.41
	Average	3.00	0.93	3.25	0.33	0.67
	Std. dev.	1.71	0.44	0.89	0.09	0.09

Table 8 (continued)

Location	Sample code	Pumice				
		Long axis (mm) (a)	Short axis (mm) (b)	a/b	b/a	OR
NEVŞEHİR	SB					
	Minimum	0.15	0.10	1.00	0.31	0.00
	Maximum	7.36	3.63	3.23	1.00	0.69
	Average	1.17	0.76	1.58	0.68	0.32
	Std. dev.	1.10	0.65	0.45	0.17	0.17
	GK					
	Minimum	0.26	0.16	1.00	0.24	0.76
	Maximum	7.52	3.59	4.20	1.00	0.00
	Average	1.36	0.86	1.61	0.67	0.33
	Std. dev.	1.13	0.66	0.54	0.17	0.17
	OH					
	Minimum	0.20	0.11	1.00	0.24	0.76
	Maximum	1.19	0.96	4.13	1.00	0.00
	Average	0.47	0.27	1.89	0.59	0.41
	Std. dev.	0.24	0.16	0.70	0.19	0.19
	KV					
	Minimum	0.15	0.09	1.00	0.14	0.00
	Maximum	1.75	0.66	7.09	1.00	0.86
	Average	0.40	0.26	1.88	0.64	0.36
	Std. dev.	0.24	0.13	1.06	0.23	0.23
	DT					
	Minimum	0.18	0.10	1.01	0.36	0.64
	Maximum	2.39	1.24	2.77	0.99	0.01
	Average	0.53	0.34	1.64	0.65	0.35
	Std. dev.	0.45	0.29	0.42	0.15	0.15
	BJ					
	Minimum	0.15	0.12	1.00	0.24	0.76
	Maximum	0.94	0.81	4.17	1.00	0.00
	Average	0.41	0.30	1.47	0.73	0.27
	Std. dev.	0.17	0.14	0.49	0.18	0.18
	BD					
	Minimum	0.20	0.08	1.07	0.29	0.71
	Maximum	1.32	0.56	3.47	0.93	0.07
	Average	0.51	0.27	2.00	0.55	0.45
	Std. dev.	0.28	0.13	0.65	0.18	0.18

Table 8 (continued)

Location	Sample code	Pumice				
		Long axis (mm) (a)	Short axis (mm) (b)	a/b	b/a	OR
AHLAT	N-1					
	Minimum	0.56	0.04	0.30	0.02	0.98
	Maximum	34.17	5.00	45.00	1.00	0.00
	Average	2.78	0.65	6.96	0.34	0.66
	Std. dev.	4.66	0.74	8.57	0.46	0.46
	N-2					
	Minimum	0.63	0.33	1.00	0.06	0.94
	Maximum	12.92	3.13	15.50	1.00	0.00
	Average	3.42	1.05	4.55	0.50	0.50
	Std. dev.	3.62	0.82	5.04	0.32	0.32
	N-3-4					
	Minimum	3.00	0.10	1.67	0.01	0.99
	Maximum	120.00	25.00	80.00	0.60	0.40
	Average	10.26	2.18	7.65	0.22	0.78
	Std. dev.	13.32	2.84	10.74	0.12	0.12

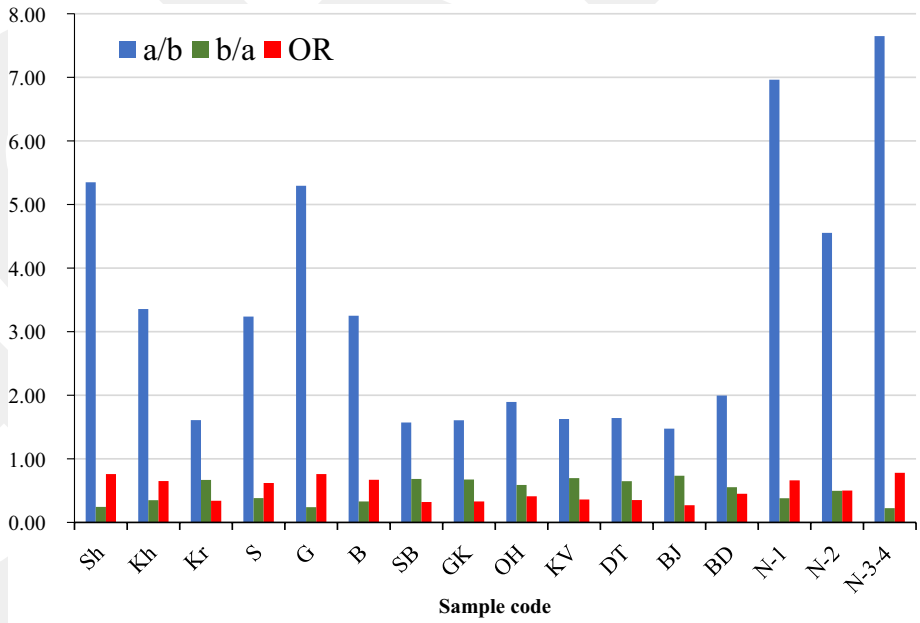

Fig. 14 Shape parameter ratios of pumice grains in the ignimbrites

(a: long axis, b: short axis)

G encoded ignimbrites, and the average aspect ratio of these samples is 0.24. An aspect ratio value of 0.66 was also obtained for the Kr coded ignimbrites. These results support that lenticular pumice grains are abundant in gray (G) and black (Sh) colored Kayseri ignimbrites. When the oblateness ratio (OR) values of the Kayseri samples are examined, it is noticed that there is not much variation between the values among the ignimbrites. While the OR value was 0.34 in Kr coded samples, the oblateness ratio in the other Kayseri ignimbrites vary between 0.62 and 0.76. Although the highest OR values are again in Sh and G coded ignimbrites, the OR values of the other ignimbrites

(except Kr) are also above 0.62. These results imply a lenticular shape of pumice grains as well (Fig. 14).

Within the scope of this research, the lowest shape parameter values of pumice grains are assigned to the Nevşehir ignimbrites. Compared to the Kayseri and Ahlat ignimbrites, the shape parameter values of the Nevşehir ignimbrites are quite low as can be seen from the column chart in Fig. 14. Low shape parameter values indicate that the pumice grains in the Nevşehir ignimbrites are more rounded. It has been determined that the average axial ratio values in the Nevşehir ignimbrites vary between 1.47 and 2.0. The highest axial ratio value for pumice grains in the Nevşehir ignimbrites was determined as 2.0 for BD coded samples. The lowest axial ratio belongs to the pumices in BJ coded Nevşehir samples. Aspect ratio (b/a) values in the Nevşehir ignimbrites range between 0.55 and 0.73. The maximum aspect ratio value of 0.73 belongs to BJ whereas an aspect ratio value of 0.55 is associated with the BD coded Nevşehir ignimbrites. Similar to the Kayseri ignimbrites, the variation of the aspect ratio values is not very wide in the Nevşehir ignimbrites. Nevertheless, it is concluded that the pumice grains in the Nevşehir ignimbrites present a more circular shape. The oblateness ratio (OR) values of 7 ignimbrite types of the Nevşehir region are between 0.27 and 0.45. Low OR values highlight that the shape of the examined pumice grains is circular.

Average shape parameter values of pumice grains of 3 different Ahlat ignimbrites (N-1, N-2, N-3-4) were investigated. Among all the ignimbrite samples evaluated within the scope of this study, the most lenticular pumice grains were determined in the Ahlat ignimbrites. In addition, the size of the pumice grains is also quite large compared to other ignimbrites. Average axial ratio (a/b), aspect ratio and oblateness ratio values in Ahlat N-1 ignimbrites were determined as 6.96, 0.34 and 0.66, respectively. In N-2 ignimbrites, these values are 4.55, 0.50 and 0.50. The highest mean axial ratio value of 7.65 is assigned to the N-3-4 sample. In these specimens, the aspect ratio is 0.22 and the oblateness ratio is 0.78. The lenticular pumice grains, which can be visually noticed on the samples, are quite characteristic for the Ahlat ignimbrites. The obtained shape parameter values also confirm the existence of lenticular fiamme structures. Furthermore, the pumice grains in the Ahlat ignimbrites are coarse and exhibit a rather elongated structure (Fig. 14).

Considering the shape parameter values, it can be concluded that the most lenticular pumice grains are in the Ahlat ignimbrites. On the other hand, the pumice grains in the Nevşehir ignimbrites are rather circular in shape. The amount of lenticular pumice grains in the Nevşehir ignimbrites is quite low. Finally, similar to the Ahlat ignimbrites, the pumice grains of the Kayseri ignimbrites are generally lenticular and elongated.

Relationship between strength of the ignimbrites and shape parameters of pumice grains

One of the most important aims of this study is to investigate the relationship between pumice grain shape and the strength of the ignimbrite samples. As it is well-known, the factors that affect the degree of welding during the formation of ignimbrites are the temperature of the pyroclastic flow and the overburden pressures that are effective on it in the depositional environment. The pumices in the pyroclastic flow exposing to high temperature and overburden load during the depositional phase acquire a lenticular shape which are called fiamme structures.

In this section, statistical relations between different shape parameters of pumice grains and uniaxial compressive strength (UCS) of the ignimbrites are presented. Figure 15 presents the statistical relationships between the average uniaxial compressive strength (dry condition) of the ignimbrites and different shape parameters for a total of 16 different ignimbrite types. Accordingly, as a result of simple regression analyses, the coefficient of determination (R2) between the uniaxial compressive strength and axial ratio (a/b) values of the ignimbrites was determined as 0.36 indicating a very poor statistical relationship.

Conversely, the coefficient of determination between the UCS values of the ignimbrites and the aspect ratio parameter of pumice is 0.61. Accordingly, it can be mentioned that there is a moderately significant negative relationship between the UCS of the ignimbrites and the b/a ratios of the pumice grains they contain. Accordingly, as the b/a ratio of pumice grains decreases, the UCS of the material increases. A similar relationship was obtained for the oblateness ratio (OR) of the pumice grains. Consequently, there is a positive relationship between UCS and the OR parameter, with a determination coefficient of 0.59. The following equations can be suggested between the aspect ratio (AR) and the oblateness ratio (OR) values of pumice in ignimbrites and their uniaxial compressive strength (UCS).

$$\mathrm{UCS} = (-33.4 * AR) + 33.9 \quad (1)$$

$$\mathrm{UCS} = (33.4 * OR) + 0.21 \quad (2)$$

Evaluation of welding degree and proposed quantitative welding classification of ignimbrites

The welding degrees of the ignimbrites examined in this study were firstly evaluated in accordance with the welding degree classification proposed by Quane and Russell (2005a). As aforementioned, the classification system of Quane and Russell (2005a) includes six different degrees

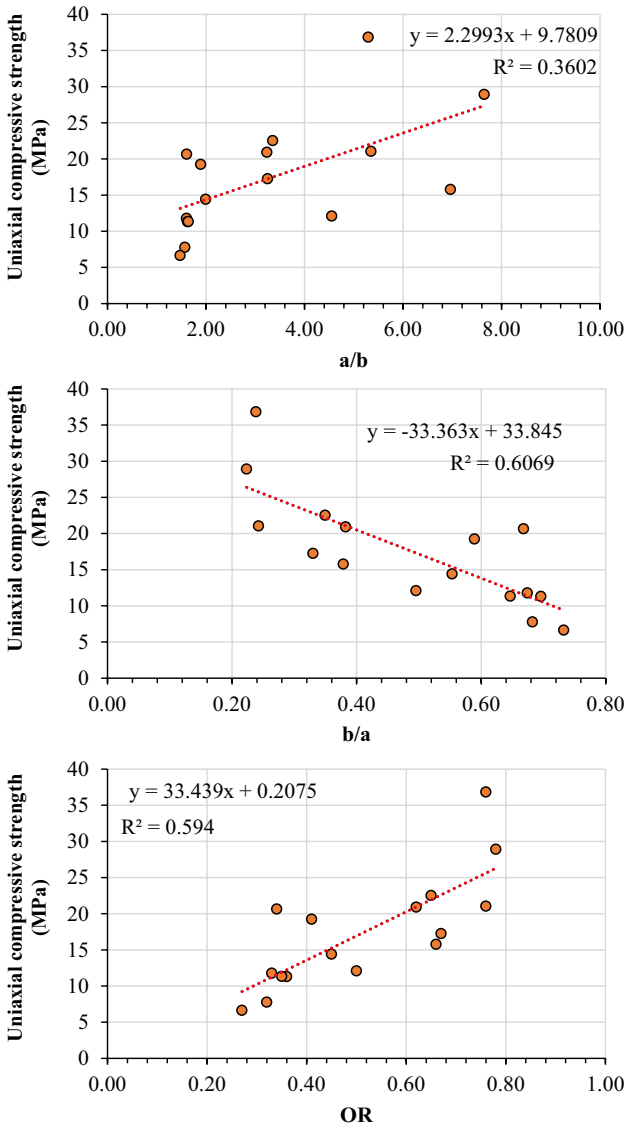

Fig. 15 Statistical relationships between the uniaxial compressive strength of the ignimbrites and the shape parameter values of pumice grains

of welding considering different physical and mechanical parameters. In Quane and Russell (2005a) classification system, class I defines unwelded ignimbrites, while class IV denotes very well welded ignimbrites. Accordingly, the welding degree classifications of 16 different ignimbrite types examined within the scope of this study, using the uniaxial compressive strength (dry), unit weight (dry), and the oblateness ratio of the pumice grains (OR, indicated as OB in the classification) are presented in Table 9.

Considering the uniaxial compressive strength parameter according to Quane and Russell (2005a) welding degree classification, it is realized that most ignimbrite specimens are in the welding degree class of III. It was determined that only Kh and G coded samples from the Kayseri ignimbrites reveal IV degree of welding. Although Nevşehir samples have very low strength, the most Nevşehir ignimbrites are in the same welding degree class with Ahlat and Kayseri samples in the welding classification based on strength (Table 9).

On the other hand, when evaluated in terms of unit weight, it is striking that the studied ignimbrites are in the welding class II, which indicates low rate of welding (Table 9). However, in general, there are obvious differences between the examined samples in terms of both strength and unit weight. Solely Kr and G coded Kayseri ignimbrites and Ahlat N-3–4 samples are in the welding degree III. Consequently, Quane and Russell (2005a) welding classification points out a lower welding degree according to unit weight than that of strength.

The Kayseri ignimbrites emerge in welding classes I, II, III and IV in the welding degree classification with respect to the oblateness ratio (OR) parameter. Conversely, all the Nevşehir ignimbrites are in welding class I considering the OR. According to the classification, the welding grade I defines ignimbrites that are weak and poorly welded with little bond among the shards. Ahlat ignimbrites are in welding class I, II and IV according to their OR values. In general, the lowest degree of welding for all samples was obtained according to the OR parameter.

As seen in Table 9, according to the welding degree classification proposed by Quane and Russell (2005a), it is determined that 16 different ignimbrite types fall into different welding degree classes according to different parameters. On the other hand, the welding classes determined by considering dry unit weight are almost the same for all sample groups (II. welding degree). Moreover, considering the uniaxial compressive strength values, it is concluded that the Nevşehir ignimbrites, which reveal very low strength, and many ignimbrite types from other regions are in the same degree of welding. Nevertheless, the Nevşehir ignimbrites exhibit significantly lower welding characteristics than the ignimbrites of the other two regions. Therefore, the Quane and Russell (2005a) welding classification has some limitations. Furthermore, the threshold values of I. and II. degree of welding classes intersects each other. For instance, while the I. degree of welding is represented by uniaxial compressive strength values lower than 4.4 MPa, the uniaxial compressive strength range is between 1.8 and 9.8 MPa for the welding degree of II involving the strength values lower than 4.4 MPa. These limitations of the Quane

Table 9 Classification of the welding degrees of the studied ignimbrites according to the average UCS, unit weight and OR parameters by means of Quane and Russell (2005a) classification

Location	Sample code	UCS (MPa)	Welding degree class	Unit weight (kN/m^3)	Welding degree class	OR	Welding degree class
KAYSERİ	Sh	21.05	III	15.71	II	0.76	III
	Kh	22.52	IV	14.64	II	0.65	II
	Kr	20.35	III	17.42	III	0.34	I
	S	20.92	III	15.37	II	0.62	II
	G	36.84	IV	17.84	III	0.76	IV
	B	17.26	III	15.78	II	0.67	II-III
NEVŞEHİR	SB	7.77	II	14.08	II	0.32	I
	GK	11.78	III	13.93	II	0.33	I
	OH	19.24	III	13.71	II	0.41	I
	KV	11.3	III	13.45	II	0.36	I
	DT	11.34	III	15.00	II	0.35	I
	BJ	6.64	II	13.86	II	0.27	I
	BD	14.41	III	14.44	II	0.45	I
AHLAT	N-1	15.78	III	15.13	II	0.66	II
	N-2	12.1	III	15.77	II	0.5	I
	N-3–4	28.92	II	16.82	III	0.78	IV

UCS Uniaxial compressive strength, *OR* Oblateness ratio

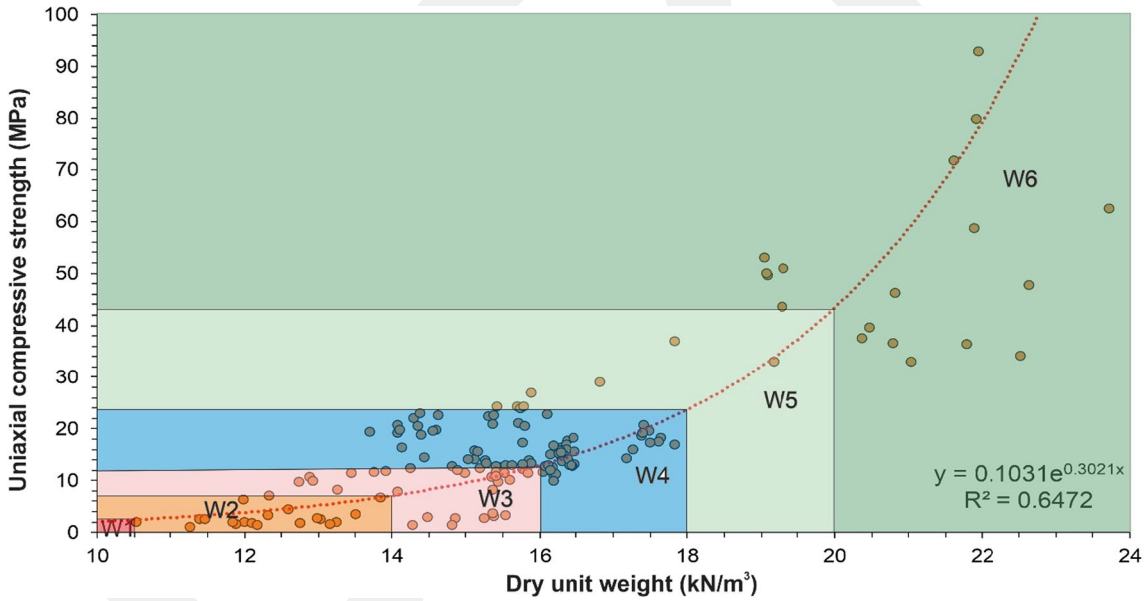

Fig. 16 Proposed quantitative welding degree classification for ignimbrites using the uniaxial compressive strength and dry unit weight

and Russell (2005a) welding classification create problems for welding evaluations.

Considering the limitations in Quane and Russell (2005a) welding degree classification, a quantitative welding degree classification is proposed for ignimbrites on the basis of the data obtained within the scope of this research as well as the experimental data from other research studies (Bostancı, 2016; Çadır, 2018; Dinçer and Bostancı, 2019; Gürbüz, 2019; Kemikkıran, 2019) carried out on several ignimbrites in the Kayseri and Nevşehir regions. In the proposed classification, the degree of welding of ignimbrites can be determined by considering the values of uniaxial compressive strength and dry unit weight (Fig. 16). The welding classification includes six different degrees of welding ranging from W1 (lowest welding degree) to W6 (highest welding degree).

Table 10 Comparison of ignimbrite welding degree class intervals proposed in this study with Quane and Russell (2005a) classification

Welding degree	This study			Welding degree	Quane ve Russell (2005)	
	Definition	UCS (MPa)	γ_d (kN/m^3)		UCS (MPa)	γ_d (gr/cm^3)
W1	Unwelded	< 2.5	< 10.5	I	< 4.4	< 1.45
W2	Very slightly welded	2.51–7.5	10.51–14.0	II	1.8–9.8	1.25–1.65
W3	Slightly welded	7.51–12.0	14.1–16.0	III	9.8–21.4	1.65–1.85
W4	Moderately welded	12.1–24.0	16.1–18.0	IV	21.4–53.2	1.85–2.15
W5	Highly welded	24.1–43.0	18.1–20.0	V	53.2–80.2	2.15–2.3
W6	Very highly welded	> 43.1	> 20.1	VI	> 80.2	> 2.3

γ_d Dry unit weight

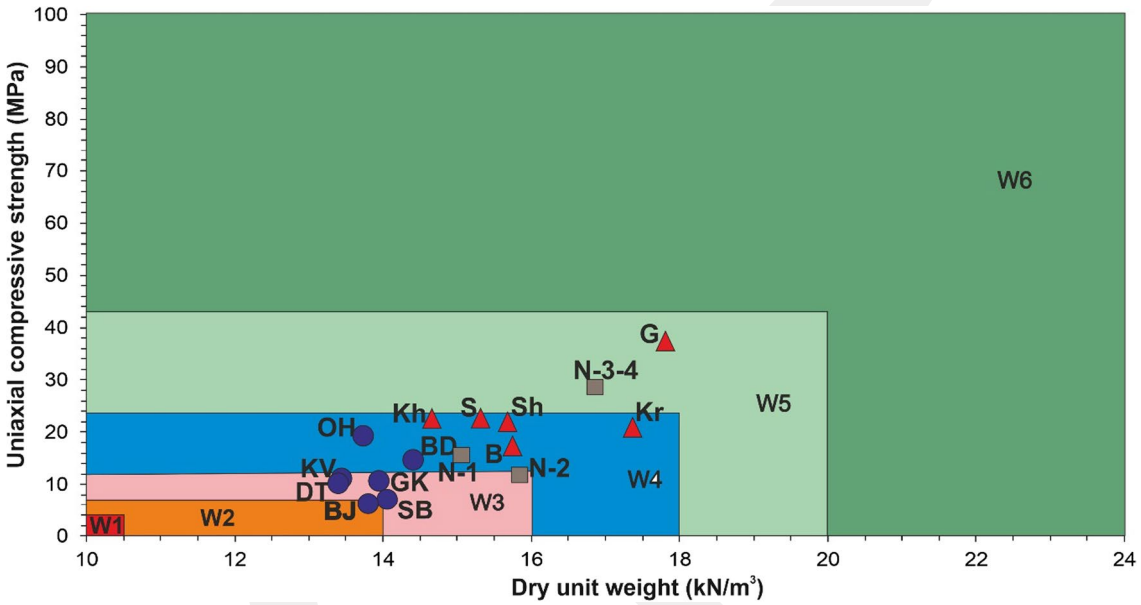

Fig. 17 Representation of the studied ignimbrites on the welding degree classification proposed in this study

The parameter threshold values of six welding classes for the proposed quantitative welding degree classification are presented in Table 10 in comparison with the value ranges of the Quane and Russell (2005a) classification. When the limit values of the two classifications are examined, it is observed that there are significant differences. In the proposed ignimbrite welding classification, the ignimbrites with uniaxial compressive strength less than 2.5 MPa were classified as unwelded (W1). In the classification of Quane and Russell (2005a), welding degree I represents unwelded ignimbrites. A significant difference between the degree of welding classification proposed in this study and the classification of Quane and Russell (2005a) is the class ranges. In the classification of the degree of welding proposed in this study, the boundary gap values in the range of welding degree of W1–W4 are narrower, while the upper limit of the degree of welding of W4 in the classification of Quane and Russell (2005a) is as high as 53.2 MPa. In the same classification, the upper dry unit weight limit for the W4 welding degree is 2.15 g/cm^3. However, ignimbrites are generally classified as low strength and low unit weight rocks. Therefore, such high strengths and unit weights in ignimbrites are the result of advanced welding. Hence, it is believed that the welding classes proposed in this study contain more practical value ranges.

In Fig. 17 and Table 11, the representation of 16 ignimbrite types examined on the proposed welding grade classification and their welding grade classes are presented. Accordingly, the Kayseri ignimbrites are dominantly classified as moderately welded (W4), except the G-coded Kayseri ignimbrite is highly welded (W5). The low strength Nevşehir ignimbrites are mostly slightly welded (W3) whereas only the BD coded ignimbrites are moderately welded (W4). Ahlat ignimbrites reveal varying degrees of welding between W3 and W5. N-3–4 ignimbrite is highly welded (W5), while N-1 ignimbrite presents moderate welding characteristics (W4). Among the Ahlat ignimbrites, the lowest degree of

Table 11 The welding degree classes of the studied ignimbrites according to the quantitative welding degree classification proposed in this study

Location	Sample code	Welding degree class	Welding degree definition
KAYSERİ	Sh	W4	Moderately welded
	Kh	W4	Moderately welded
	Kr	W4	Moderately welded
	S	W4	Moderately welded
	G	W5	Highly welded
	B	W4	Moderately welded
NEVŞEHİR	SB	W3	Slightly welded
	GK	W3	Slightly welded
	OH	W4	Moderately welded
	KV	W3	Slightly welded
	DT	W3	Slightly welded
	BJ	W3	Slightly welded
	BD	W4	Moderately welded
AHLAT	N-1	W4	Moderately welded
	N-2	W3	Slightly welded
	N-3–4	W5	Highly welded

Table 12 Threshold values of pumice grain oblateness ratio (OR) for the suggested ignimbrite welding degree classes

Welding degree class	Definition	Oblateness ratio (OR)
W1	Unwelded	< 0.09
W2	Very slightly welded	0.091–0.21
W3	Slightly welded	0.211–0.35
W4	Moderately welded	0.351–0.71
W5	Highly welded	0.711–0.8
W6	Very highly welded	> 0.81

welding is in N-2 ignimbrites, which are slightly welded (W3).

Finally, in order to present the relationship between the degree of welding of ignimbrites and the oblateness ratio (OR) of the pumice grains, the threshold values of the oblateness ratio for each welding class in the proposed welding degree classification were also determined Accordingly, the pumice grain oblateness ratio (OR) distributions for the proposed ignimbrite welding classes are depicted in Table 12. Furthermore, the welding degree classes according to the OR values of the examined ignimbrites are compared with the welding degree classes with respect to uniaxial compressive strength and dry unit weight (Table 13).

When Table 13 is examined, it is obvious that there is a great similarity (12 out of 16) between the welding degree classes determined by means of the proposed welding degree classification for the ignimbrites (by using uniaxial compressive strength and dry unit weight parameters) and the classification made by the pumice grains' oblateness ratio (OR). The degree of welding depending on the UCS and γ_d values and the degree of welding determined by considering the oblateness ratio values are significantly consistent.

Table 13 The welding degree classes of the investigated ignimbrites according to the oblateness ratio (OR) and UCS-γ_d

Location	Sample code	Welding degree class according to UCS and γ_d	Welding degree class according to OR
KAYSERİ	Sh	W4	W5
	Kh	W4	W4
	Kr	W4	W3
	S	W4	W4
	G	W5	W5
	B	W4	W4
NEVŞEHİR	SB	W3	W3
	GK	W3	W3
	OH	W4	W4
	KV	W3	W4
	DT	W3	W3
	BJ	W3	W3
	BD	W4	W4
AHLAT	N-1	W4	W4
	N-2	W3	W4
	N-3–4	W5	W5

Discussions and conclusions

Within the scope of this study, the petrographical, geochemical, physical and mechanical properties of the ignimbrites with different color, texture and strength properties obtained from three different regions (Kayseri, Nevşehir, and Ahlat) where ignimbrite rocks are commonly observed in Turkey were examined. The shape ratios of the grains were determined according to different shape parameter evaluation methods. As one of the most important aims of the research, the relationships between the degree of welding of the ignimbrites and the shape of the pumice grains were examined according to the physical and mechanical properties as well as shape parameter values.

As a result of the petrographic analyses, it was determined that the examined ignimbrites present regional differences in terms of type and abundance of the components (phenocrystal, lithic and pumice fragments and volcanic glass). All ignimbrites reveal hypohyaline porphyritic texture. They contain volcanic glass shards and/or pumice fragments as glass component. According to

the Schmid (1981) classification, Sh, Kh, S, B and G samples of ignimbrites in the Kayseri region were classified as vitric tuff and Kr sample as lithic tuff. Similarly, all the Nevşehir ignimbrites (SB, GK, BJ, OK, KV, DT and BD) were classified as vitric tuff. Finally, the Ahlat ignimbrites were also defined as vitric tuff according to the Schmid (1981) classification. It is noticeable that the pumice grains in Kayseri and Ahlat regions generally present fiamme structures.

According to the ANON (1979) classification, it was determined that the unit weight of all ignimbrites is very low unit weight. Dry and saturated unit weight values of the ignimbrites belonging to Kayseri and Ahlat regions are very close. Besides, it was revealed that the Kayseri and Ahlat ignimbrites have high porosity according to the ANON (1979) classification, while the Nevşehir ignimbrites are very highly porous. Most ignimbrite samples present a P-wave velocity lower than 2500 m/s representing a very low velocity. The Kayseri ignimbrites are classified as medium strong rocks. On the other hand, the Nevşehir and Ahlat ignimbrites are weak rocks with the exception of OH, N-1 and N-3–4 coded samples.

A number of the Kayseri ignimbrites lose more than 30% of their strength under saturated conditions. Similarly, uniaxial compressive strength of the Nevşehir ignimbrites significantly decreases in contact with water. There is no noteworthy reduction in strength under saturated conditions for the Ahlat ignimbrites. These outcomes indicate that especially the Kayseri and Nevşehir ignimbrites may drastically lose their strength in contact with surface water.

Considering the shape parameter values of the pumice grains in the ignimbrites, it can be concluded that the most lenticular pumice grains are in the Ahlat ignimbrites. On the other hand, the pumice grains in the Nevşehir ignimbrites are rather circular in shape. The amount of lenticular pumice grains in these ignimbrites is quite low. Similar to the Ahlat ignimbrites, the pumice fragments in the Kayseri ignimbrites are generally lenticular and elongated. As expected, the pumice grains in the ignimbrites were flattened as a result of temperature and pressure at the time of deposition.

Within the scope of this research, statistical relationships between different shape parameters of pumice fragments and uniaxial compressive strength of ignimbrites were investigated. As a result of statistical evaluations, the coefficient of determination between the UCS values of the ignimbrites and the aspect ratio parameter of pumice is 0.61. In other words, as the b/a ratio (aspect ratio) of the pumice grains decreases, the UCS of the material increases. A similar relationship was obtained for the oblateness ratio (OR) of the pumice grains. Accordingly, there is a positive relationship between UCS and the OR parameter, and the coefficient of determination of this statistical relationship was found to be 0.59.

As a result of Quane and Russell (2005a) welding classification by considering uniaxial compressive strength, unit weight and oblateness ratio (OR) of pumice grains for 16 different ignimbrite types, different welding degrees were assigned to each ignimbrite according to different parameters. Similarly, another welding degree classification of ignimbrites suggested by Selçuk and Beyaz (2021) reveal varying welding degree values to the investigated specimens specifically for the low strength ignimbrites. For instance, SB and BJ coded Nevşehir samples which have the lowest strength are classified as sintered (class II) in accordance with Selçuk and Beyaz (2021) classification, both specimens are accepted as very poor welded due to the dry unit weight values.

One of the major limitations of the Quane and Russell (2005a) as well as Selçuk and Beyaz (2021) classifications are that each parameter can express a different degree of welding as these parameters are considered individually. Considering the uniaxial compressive strength parameter in Quane and Russell (2005a) welding degree classification, it is defined that most of the studied ignimbrite samples are in the III. welding degree class. Although the Nevşehir ignimbrites have lower strength and unit weight, most of the Nevşehir ignimbrites were included in the same welding class with Ahlat and Kayseri samples in the welding classification based on strength. Considering the limitations in the welding classifications proposed by Quane and Russell (2005a) and Selçuk and Beyaz (2021), a double-parameter quantitative welding degree classification for ignimbrites is proposed as a result of this research. In this welding degree classification, welding of ignimbrites can be determined considering the uniaxial compressive strength and dry unit weight values, and the classification includes six different welding degrees ranging from W1 (unwelded) to W6 (very highly welded).

The degree of welding of 16 ignimbrite types was evaluated according to the newly proposed quantitative welding classification. Accordingly, the Kayseri ignimbrites are classified as moderately welded ignimbrites (W4), except for G-coded specimens (W5). The Nevşehir ignimbrites are mostly slightly welded (W3). Moreover, the Ahlat ignimbrites have varying degrees of welding between W3 and W5. N-3–4 ignimbrite is highly welded (W5), while the welding degree of N-1 ignimbrite is moderate (W4). Among the Ahlat ignimbrites, the lowest degree of welding (W3) is assigned to N-2 specimens.

To express the relationship between degree of welding of the ignimbrites and the oblateness ratio (OR) of the pumice grains, the threshold values of the oblateness ratio for the welding classes in the proposed classification were also determined. A great deal of similarity was found

between the welding degree classes of ignimbrites and pumice grains' oblateness ratio (OR). The results indicate that the welding degree classification proposed for ignimbrites is highly compatible with the experimental as well as observational studies. The simultaneous consideration of a couple of parameters (UCS and dry unit weight) in the proposed classification enhances the quantitative evaluation of the degree of welding.

Acknowledgements This study was financially supported by the Scientific Research Projects Coordination Office of the Nevşehir Hacı Bektaş Veli University (project number BAP18F25). We deeply thank the Nevşehir Hacı Bektaş Veli University Scientific Research Projects Coordination Office for the financial support.

Author contributions Authors Mutluhan Akin, Tamer Topal, İsmail Dinçer, Muge K. Akin and Ayse Orhan wrote the main manuscript text. The figures are prepared by Muge K. Akin, Ayse Orhan, Ali Ozvan and Mutluhan Akin. The laboratory tests were performed by Mutluhan Akin, İsmail Dinçer, Ahmet Orhan and Ali Ozvan. All authors reviewed the manuscript.

Funding Nevşehir Hacı Bektaş Veli Üniversitesi, BAP18F25.

Declarations

Competing interests The authors declare no competing interests.

References

ANON (1979) Classification of rocks and soils for engineering geological mapping part 1: rock and soil materials. Bull Int Assoc Eng Geol 19:355–371

Bostancı,M. (2016) İgnimbiritlerin (Nevşehir Bölgesi) Kapiler Su Emme Davranışlarının İncelenmesi. Nevşehir Hacı Bektaş Veli Üniversitesi, Fen Bilimleri Enstitüsü, Yüksek Lisans Tezi, 79 sayfa (in Turkish).

Bozdağ A, Bayram AF, İnce İ, Asan K (2016) The relationship between weathering and welding degree of pyroclastic rocks in the Kilistra ancient city, Konya (Central Anatolia, Turkey). J Afr Earth Sc 123:1–9

Braney MJ, Kokelaar P (1992) A reappraisal of ignimbrite emplacement: progressive aggradation and changes from particulate to non-particulate flow during emplacement of high-grade ignimbrite. Bull Volcanol 54:504–520

Çadır S (2018) Piroklastik Kayaçlarda Mikro-Yapının Fiziksel ve Mekanik Özellikler Üzerine Etkisi. Nevşehir Hacı Bektaş Veli Üniversitesi, Fen Bilimleri Enstitüsü, Yüksek Lisans Tezi, 91 sayfa (in Turkish).

Deer WA, Howie RA, Zussman J (1992) An Introduction to the Rock-forming Minerals. Longman Scientific and Technical, ISBN 0470218096. pp 696.

Dinçer İ, Bostancı M (2019) Capillary water absorption characteristics of some Cappadocian ignimbrites and the role of capillarity on their deterioration. Environ Earth Sci 78:7

Freundt A, Schmincke HU (1995) Eruption and emplacement of a basaltic welded ignimbrite during caldera formation on Gran Canaria. Bull Volcanol 56:640–659

Gifkins CC, Allen RL, McPhie J (2005) Apparent welding textures in altered pumice-rich rocks. J Volcanol Geoth Res 142:29–47

Gürbüz, S., 2019. Nevşehir Yöresindeki İgnimbiritlerin Dayanımının Tahmininde Schmidt Geri Sıçrama Değerlerinin Kullanımı. Nevşehir Hacı Bektaş Veli Üniversitesi, Fen Bilimleri Enstitüsü, Yüksek Lisans Tezi, 59 sf (in Turkish).

ISRM, 2007. The Complete ISRM Suggested Methods for Rock Characterization, Testing and Monitoring: 1974–2006. Suggested Methods Prepared by the Commission on Testing Methods, International Society for Rock Mechanics, Compilation Arranged by the ISRM Turkish National Group Ankara, Turkey. pp 628.

Kemikkıran, Ö., F., 2019. Nevşehir Yöresindeki İgnimbiritlerin Fiziksel ve Mekanik Özellikleri ile P-dalga Hızı Arasındaki İlişkilerin İncelenmesi. Nevşehir Hacı Bektaş Veli Üniversitesi, Fen Bilimleri Enstitüsü, Yüksek Lisans Tezi, 79 sf (in Turkish).

Koralay T, Özkul M, Kumsar H, Çelik SB, Pektaş K (2011) The effect of welding degree on geotechnical properties of an ignimbrite flow unit: the Bitlis castle case (Eastern Turkey). Environ Earth Sci 64:869–881

Korkanç M, Solak B (2016) Estimation of engineering properties of selected tuffs by using grain/matrix ratio. J Afr Earth Sc 120:160–172

Leake BE, Woolly AR, Arps CES, Birch WD, Gilbert MC, Grice JD, Hawthorne FC, Kato A, Kisch HJ, Krivovichev VG (1997) Nomenclature of Amphiboles. Report of the Subcommittee on Amphiboles of the International Mineralogical Association Commission on New Minerals Names, European. J Mineral 9:623–651

Lindsley DH, Andersen DJ (1983) A two pyroxene thermometer. J Geophys Res 88:887–906

Luhr JF, Carmichael ISE, Varekamp JC (1984) The 1982 eruptions of El Chicón Volcano, Chiapas, Mexico: mineralogy and petrology of the anhydrite-bearing pumices. J Volcanol Geoth Res 23:69–108

Middlemost EAK (1994) Naming materials in the magma/igneous rock system. Earth Science Review 37:215–244

Moon VG (1993) Microstructural controls on the geomechanical behaviour of ignimbrite. Eng Geol 35:19–31

Morimoto MJ, Fabries AK, Ferguson IV, Ginzburg M, Ross FA (1988) Nomenclature of pyroxenes. Mineral Mag 52:535–550

Mues-Schumacher U, Schumacher R, Viereck-Götte G, Lepetit P (2004) Areal distribution and bulk rock density variations of the welded İncesu ignimbrite, Central Anatolia. Turkey. Turk J Earth Sci. 13:249–267

Mundula F, Cioni R, Rizzo R (2009) A simplified scheme for the description of textural features in welded ignimbrites: the example of San Pietro Island (Sardinia, Italy). Ital. J. Geosci. 128(3):615–627

Pola A, Macías J, Crosta G, Fusi N, Martinez-Martinez J (2016) Geomechanical characterization of different lithofacies of the Cuitzeo ignimbrites. Eng Geol 214:79–93

Putirka KD (2008) Introduction to minerals, inclusions and volcanic processes. Rev Mineral Geochem 69:1–8

Quane SL, Russell JK (2005a) Ranking welding intensity in pyroclastic deposits. Bull Volcanology 67:129–143

Quane SL, Russell JK (2005b) Welding: insights from high-temperature analogue experiments. J Volcanol Geoth Res 142:67–87

Ridolfi F (2021) Amp-TB2: an updated model for calcic amphibole thermobarometry. Minerals 11(3):324

Schmid R (1981) Descriptive nomenclature and classification of pyroclastic deposits and fragment: recommendations of the IUGS subcommissions on the systematics of igneous rocks. Geology 9:41–43

Selçuk L, Beyaz T (2021) Welding intensity assessment of pyroclastic units based on engineering quality requirements. Arab J Geosci 14:382

Sheridan MF, Ragan DM (1976) Compaction of ash-flow tuffs. In: Chilingarian GV, Wolf KH (eds) Compaction of coarse-grained sediments, II. Elsevier, Amsterdam, pp 677–717

Smith RL (1960) Zones and Zonal variations in welded ash flows. U.S. Geol. Survey Prof. Paper 354:149–159
Streck MJ, Grunder AL (1995) Crystallization and welding variations in a widespread ignimbrite sheet: the Rattlesnake Tuff, eastern Oregon, USA. Bull Volcanol 57:151–169
Tischendorf G, Gottesmann B, Forster HJ, Trumbull RB (1997) On Li-bearing micas: estimating Li from electron microprobe analysis and an improved diagram for graphical representation. Mineral Mag 61:809–834
Tran NH (2007) Fracture orientation characterization: minimizing statistical modelling errors. Comput Stat Data Anal 51(6):3187–3196
Walker GPL (1983) Ignimbrite types and ignimbrite problems. J Volcanol Geotherm Res 17:65–88